GMI assessments of Aerosol–Cloud-Climate Interactions

Rafaella P. Sotiropoulou and Athanasios Nenes

Georgia Institute of Technology

GMI Science Meeting
June 13-15, 2007

Acknowledgements: NASA NIP, NASA IDS

GMI: Aerosol-Cloud-Climate Interactions

Currently Accomplished:

- Implementation of aerosol-cloud interaction modules:
  - Cloud-relevant parameters changes with meteo-fields used.
  - Meteo-fields currently used: DAO, GISS, GEOS-4.
- Cloud properties are calculated from parameterizations.
- Implemented droplet formation parameterizations:
  - Boucher and Lohmann, 1995 (**BL**) – empirical
  - Abdul-Razzak & Ghan, 2000 (**AG**) - mechanistic
  - Nenes & Seinfeld,2003; Fountoukis & Nenes,2005 (**FN**) – mechanistic
  - Segal & Khain, 2006 (**SK**) - empirical
- Assessments of indirect effect and autoconversion rate using various droplet formation parameterization and meteorology.
- U of Michigan, AEROCOM aerosol emission scenarios.

GMI Improvements:

- ✓ Effective radius $r_e = k\left(\frac{3}{4}\frac{\rho_a q_l}{\pi \rho_w b N_d}\right)^{1/3}$ k=1.143 (Cont); k=1.077 (Mar) (Martin et al., 1994)
- ✓ Cloud optical depth $\tau_C = \frac{3}{2}\frac{LWC\ h}{\rho_w r_e}$ (Seinfeld & Pandis, 1998)
- ✓ Subgrid cloud optical depth variability $\tau = \tau_C C^{3/2}$ (Briegleb, 1992)
- ✓ Cloud albedo $R_c = \frac{\tau}{\tau + 7.7}$ (Seinfeld & Pandis, 1998)
- ✓ Radiative transfer module for shortwave (SW) radiative fluxes
- ✓ Solar radiation transmitted through each vertical layer:

$$I_i = I_i^{att}(1-\alpha_i)$$

✓ Autoconversion rate:

3 schemes are used [Kharoutdinov & Kogan, 2000; Rotstayn, 1997]:

Autoconversion rate

Cloud fraction

LWMR

Cloud droplet number

$$(\dot{q}_l)_{AU} = 1350\ C_l q_c^{2.47} N_d^{-1.79} \qquad (1)$$

Mean volume radius

$$(\dot{q}_l)_{AU} = 4.1\times 10^{15}\, C_l r_v^{5.67} \qquad (2)$$

Mean collection efficiency

$$(\dot{q}_l)_{AU} = -C_l \frac{0.104\, g E_{AU} \rho^{\frac{4}{3}}}{\mu (N_d \rho_w)^{\frac{1}{3}}} \left(\frac{q_l}{C_l}\right)^{\frac{7}{3}} H\left(\frac{q_l}{C_l} - q_{CR}\right) \qquad (3)$$

Dynamic viscosity of air

Critical LWMR

CDNC Calculation – Empirical Schemes

Bypass complex physics of droplet formation

Boucher & Lohmann (1995)

The scheme is based on simultaneous measurements of sulfate and either cloud condensation nuclei (CCN) or CDNC.

$$N_d = \begin{cases} 10^{2.06+0.48\log\left(m_{SO_4}\right)} & \text{over oceans} \\ 10^{2.24+0.257\log\left(m_{SO_4}\right)} & \text{over land} \end{cases}$$

m_{SO_4} (μg m^{-3}) specified from GMI

Segal & Khain (2006)

CDNC calculation is based on regression equation that expresses the dependence of CDNC on the cloud nuclei (CN) concentration, on the parameters of the CN size distribution and on the vertical velocity at the cloud base.

$$\begin{aligned} N_d = {} & b_0 + b_1\frac{W_{cb}-\overline{W}_{cb}}{\sigma_W} + b_2\frac{\log(N_{CN})-\log(\overline{N}_{CN})}{\sigma_{\log(N_{CN})}} + b_3\frac{W_i-\overline{W}_i}{\sigma_{W_i}} \\ & + b_{11}\left(\frac{W_{cb}-\overline{W}_{cb}}{\sigma_W}\right)^2 + b_{22}\left(\frac{\log(N_{CN})-\log(\overline{N}_{CN})}{\sigma_{\log(N_{CN})}}\right)^2 + b_{33}\left(\frac{W_i-\overline{W}_i}{\sigma_{W_i}}\right)^2 \\ & + b_{12}\left(\frac{W_{cb}-\overline{W}_{cb}}{\sigma_W}\right)\left(\frac{\log(N_{CN})-\log(\overline{N}_{CN})}{\sigma_{\log(N_{CN})}}\right) + b_{13}\left(\frac{W_{cb}-\overline{W}_{cb}}{\sigma_W}\right)\left(\frac{W_i-\overline{W}_i}{\sigma_{W_i}}\right) \\ & + b_{23}\left(\frac{\log(N_{CN})-\log(\overline{N}_{CN})}{\sigma_{\log(N_{CN})}}\right)\left(\frac{W_i-\overline{W}_i}{\sigma_{W_i}}\right) \end{aligned}$$

CDNC Calculation – Physically Based Schemes

Abdul-Razzak & Ghan (1998; 2000)

- For lognormal aerosol models
- Computationally efficient
- Kinetic limitations and the influence of surfactants on the activation process are neglected

Nenes & Seinfeld (2003); Fountoukis & Nenes (2005)

- For lognormal and sectional aerosol models
- Computationally efficient.
- Can treat very complex internal/external aerosol, and effects of organic films on droplet growth kinetics.
- In-situ validation for a wide range of stratocumulus and cumulus clouds, clean and polluted (Meskhidze *et al.*, JGR, 2005; Fountoukis *et al.*, JGR, 2007)
- Extensive intercomparison with other parameterizations shows that it outperforms them for wide range of conditions (1000's of data points).

Simulations Considered

Emission Scenarios

- University of Michigan (Present day, Preindustrial)
- AEROCOM (Present day, Preindustrial)

Base Case Simulations

- Liquid Cloud Temperatures: 273 K and above
- Cloud droplet formation schemes: BL and FN

Sensitivity examined

- Cloud temperatures:
  263 K over land, 269 K over ocean (GISS GCM scheme)
- Cloud droplet formation schemes: BL, SK, AG, FN

Total Number of Simulations (for now):

$$\overbrace{4 \times 3 \times 2 \times 2}^{\text{U of Michigan}} + \overbrace{1 \times 2}^{\text{AEROCOM}} = 50$$

N_d scheme — Met field — Threshold T — Emission Case — Met field — Emission Case

Some results:
"Base Case" Simulations

(i.e., Liquid Cloud Temperatures: 273 K and above, BL and FN cloud droplet formation schemes.)

Cloud Droplet Number (cm^{-3}) (annual average)

Conditions:

Prescribed updrafts (marine: 0.35 ms^{-1}; continental: 1 ms^{-1})

Water vapor mass uptake coefficient, a_c = 0.042 (FN)

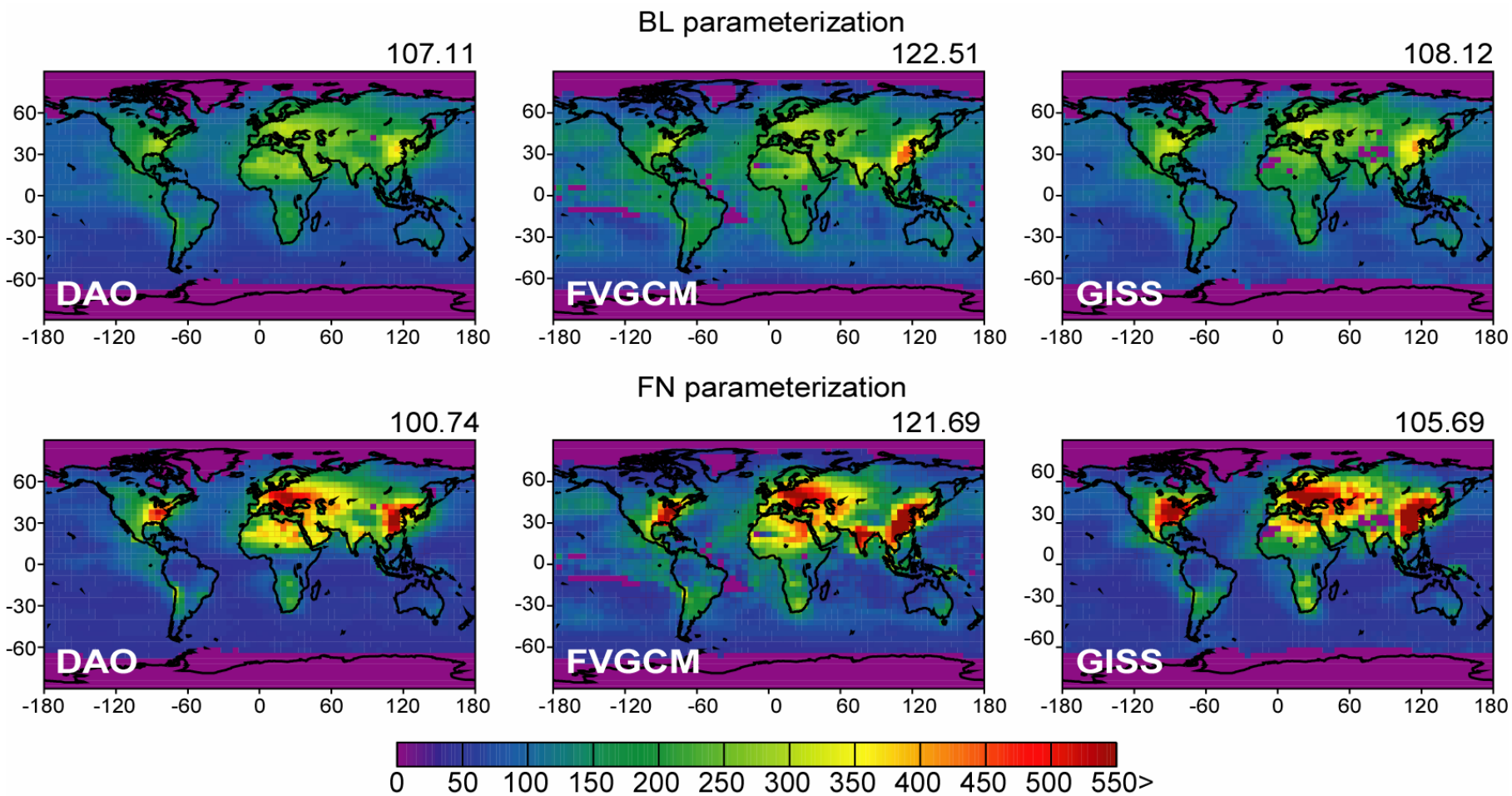

Droplet Effective Radii (μm)

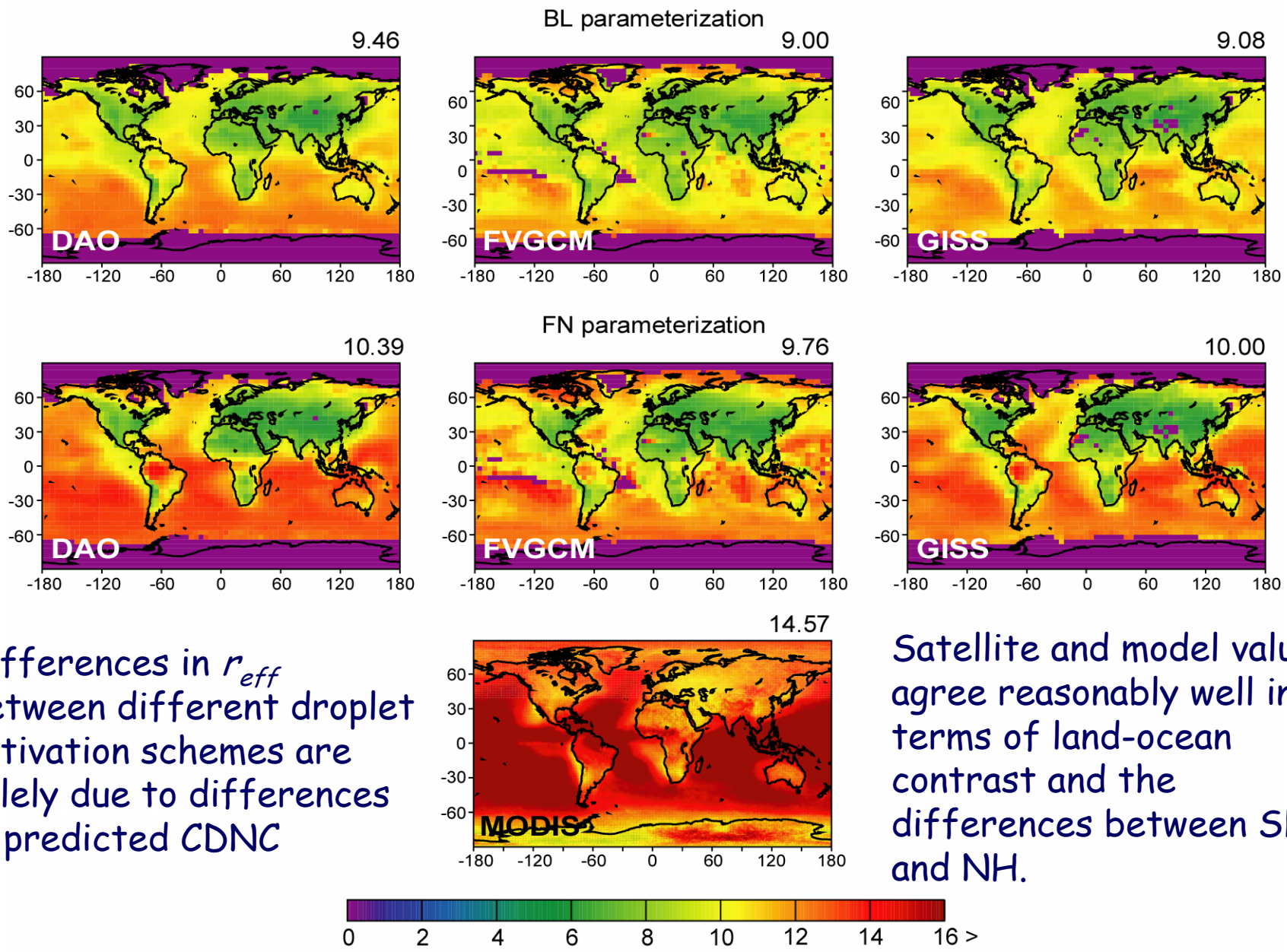

Differences in r_{eff} between different droplet activation schemes are solely due to differences in predicted CDNC

Satellite and model values agree reasonably well in terms of land-ocean contrast and the differences between SH and NH.

Cloud Optical Thickness (τ)

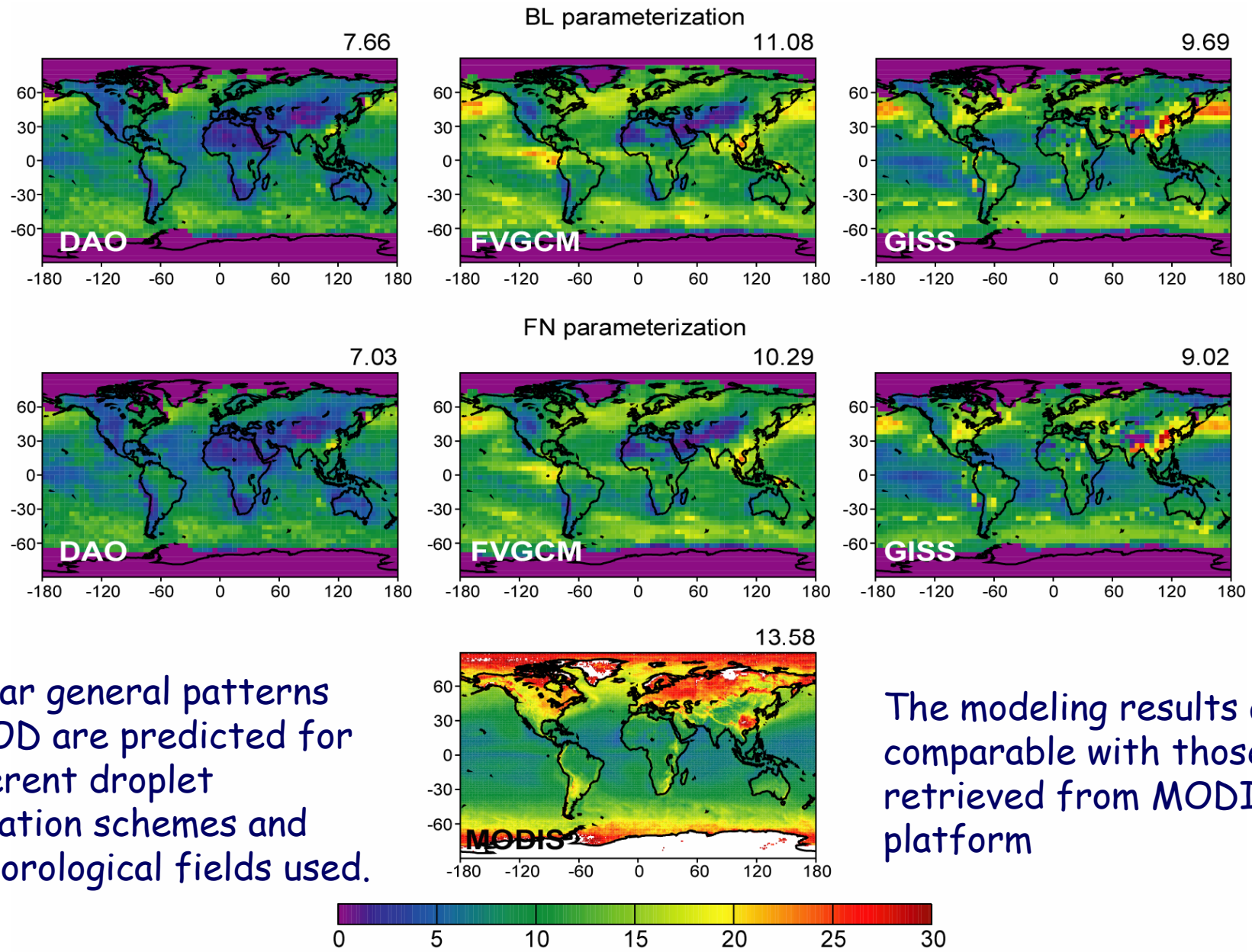

Similar general patterns of COD are predicted for different droplet activation schemes and meteorological fields used.

The modeling results are comparable with those retrieved from MODIS platform

Model Evaluation with Satellite Observations

R_{eff} (μm)	DAO		FVGCM		GISS		ISCCP[1]	MODIS[2]
	FN	BL	FN	BL	FN	BL		
Ocean	12.24	11.03	10.98	9.95	11.80	10.56	11.8	**15.6**
NH Ocean	11.36	10.11	10.25	9.35	11.19	9.92	11.6	**15.4**
SH Ocean	12.92	11.72	11.51	10.38	12.28	11.03	12.0	**15.8**
Land	8.93	8.44	8.65	8.39	8.53	8.16	8.5	**12.5**
NH Land	8.45	8.19	8.27	8.18	8.06	7.87	8.2	**12.4**
SH Land	10.96	9.62	10.02	9.14	10.47	9.40	9 .0	**13.1**

COD	DAO		FVGCM		GISS		ISCCP[1]	MODIS[2]
	FN	BL	FN	BL	FN	BL		
Ocean	8.38	9.19	11.45	11.76	9.42	10.26	6.9	**11.2**
NH Ocean	7.53	8.38	12.04	11.99	9.24	10.15	6.4	**10.7**
SH Ocean	8.89	9.67	10.95	11.55	9.38	10.14	7.4	**11.5**
Land	5.82	6.19	9.57	7.93	10.74	11.15	8.1	**15.7**
NH Land	5.87	6.13	9.71	7.76	11.04	11.24	7.8	**16.7**
SH Land	5.88	6.70	9.53	8.95	9.70	10.82	8.6	**13.0**

1) Values are taken from *Han et al.* [1994].
2) MODIS Terra Collection 005 (C5) Level-3 global gridded monthly averaged products at 1° by 1° resolution for April 2000 – December 2006 were used. To minimize data contamination by ice particles, data were averaged between 70°S to 70°N.

Model Evaluation with Satellite Observations

Land/Ocean Contrast

R_{eff} (μm)	DAO		FVGCM		GISS		ISCCP	MODIS
	FN	BL	FN	BL	FN	BL		
Land/Ocean	0.73	0.77	0.79	0.84	0.72	0.77	0.72	0.80
NH Land/Ocean	0.74	0.81	0.81	0.87	0.72	0.79	0.71	0.81
SH Land/Ocean	0.85	0.82	0.87	0.88	0.85	0.85	0.75	0.83

COD	DAO		FVGCM		GISS		ISCCP	MODIS
	FN	BL	FN	BL	FN	BL		
Land/Ocean	0.69	0.67	0.84	0.67	1.14	1.09	1.17	1.40
NH Land/Ocean	0.78	0.73	0.81	0.65	1.19	1.11	1.22	1.56
SH Land/Ocean	0.66	0.69	0.87	0.77	1.03	1.07	1.16	1.13

This is roughly indicative of the model's ability to capture the indirect effect (especially when you are comparing for the NH land vs. ocean contrast).

Comparison with online GISS II' GCM simulation

In the group we also work with the GISS GCM with online aerosol; both mass-based only (Sotiropoulou et al., 2007) and with TOMAS microphysics (Adams and Seinfeld, 2002).

It is important to see how well the GMI simulation, with offline GISS metfields, compares to the GISS climate model simulation with online aerosol (both are run with fixed SST's and reproduce the general climatology).

Parameter	GISS II'			GMI		
	Present day	Pre industrial	Absolute change from pre industrial	Present day	Pre industrial	Absolute change from pre industrial
CDNC	98.82	41.76	138%	98.08	44.66	120%
COD	8.76	7.97	10%	8.42	7.41	14%

The agreement between the two models is remarkable!!!
We are doing a good job.

Annual Mean First Indirect Forcing (W m^{-2})

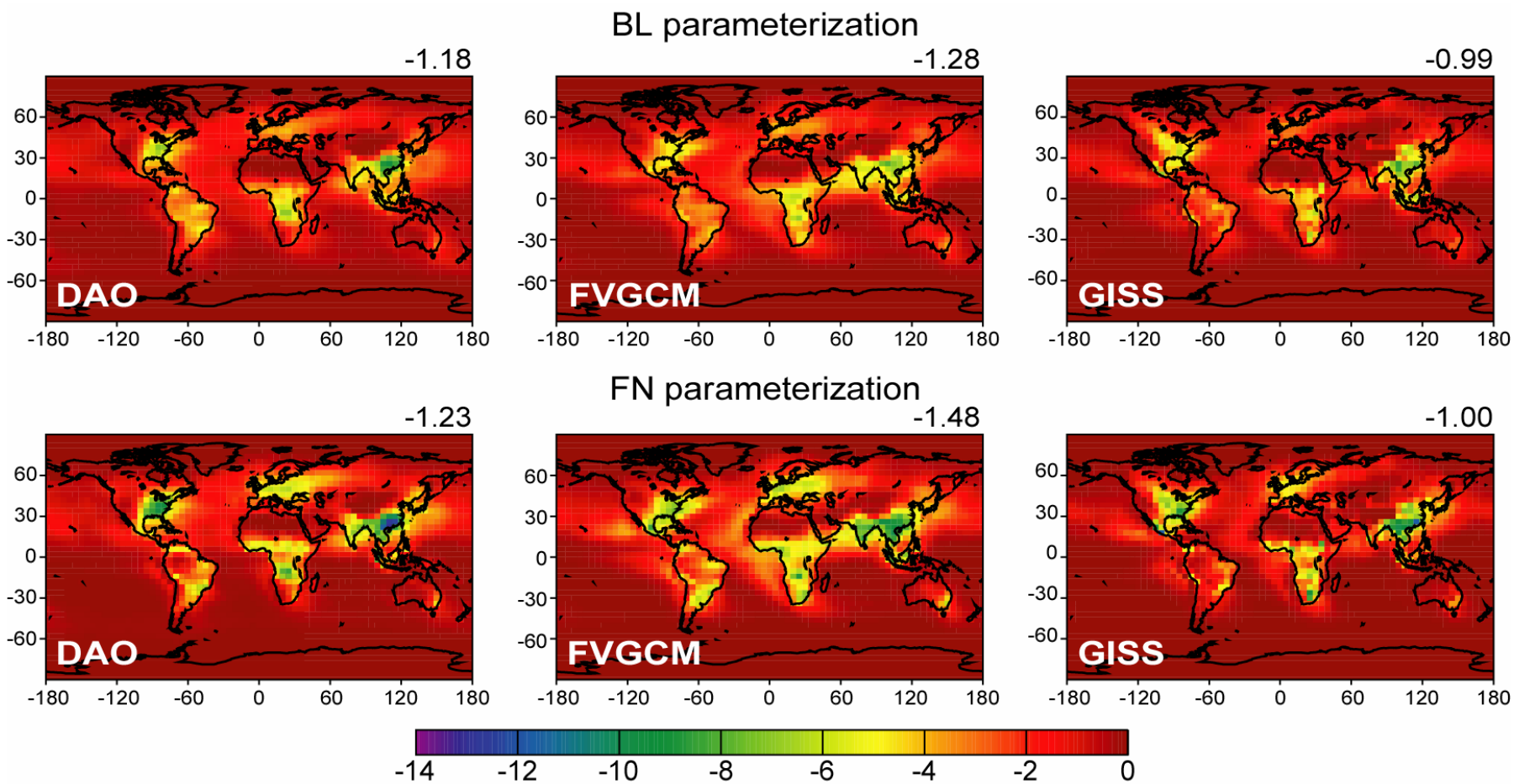

The spatial patterns of indirect forcing follow that of CDNC

Range: -0.99 to -1.48 Wm^{-2}

Annual Mean Autoconversion Rate ($\times 10^{11}$ s^{-1})

Conditions: Eq.1 of Kharoutdinov and Kogan, 2000

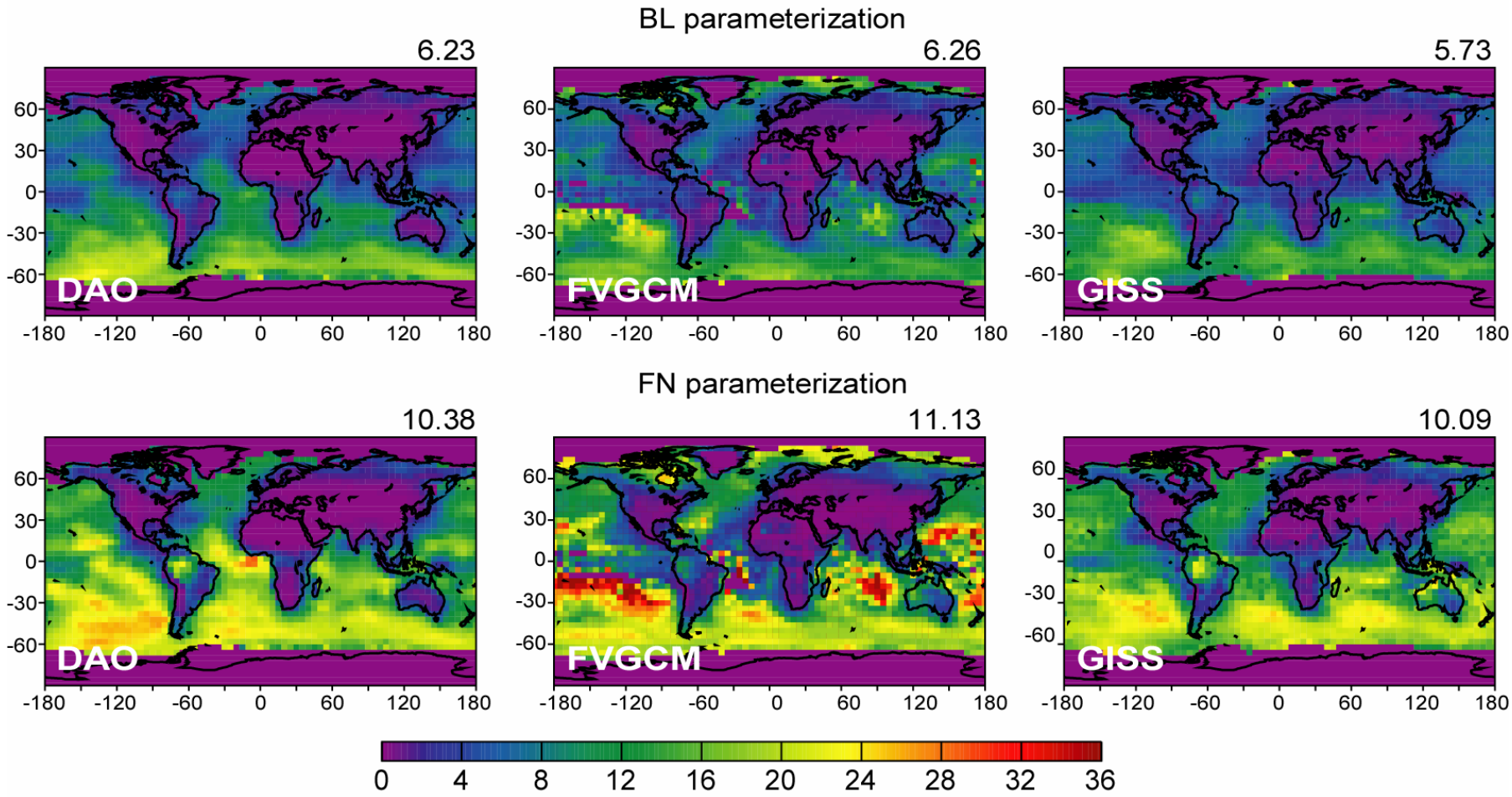

Spatial patterns anticorrelated with CDNC

Autoconversion much more sensitive to parameterization than AIF

More (interesting) results: "Sensitivity" Simulations

(i.e., Change Liquid Cloud Temperature Threshold, more droplet schemes.)

Cloud Droplet Number (cm^{-3}) (annual average)

Conditions:

Prescribed updrafts (marine: 0.35 ms^{-1}; continental: 1 ms^{-1})

Water vapor mass uptake coefficient, a_c = 0.042 (FN)

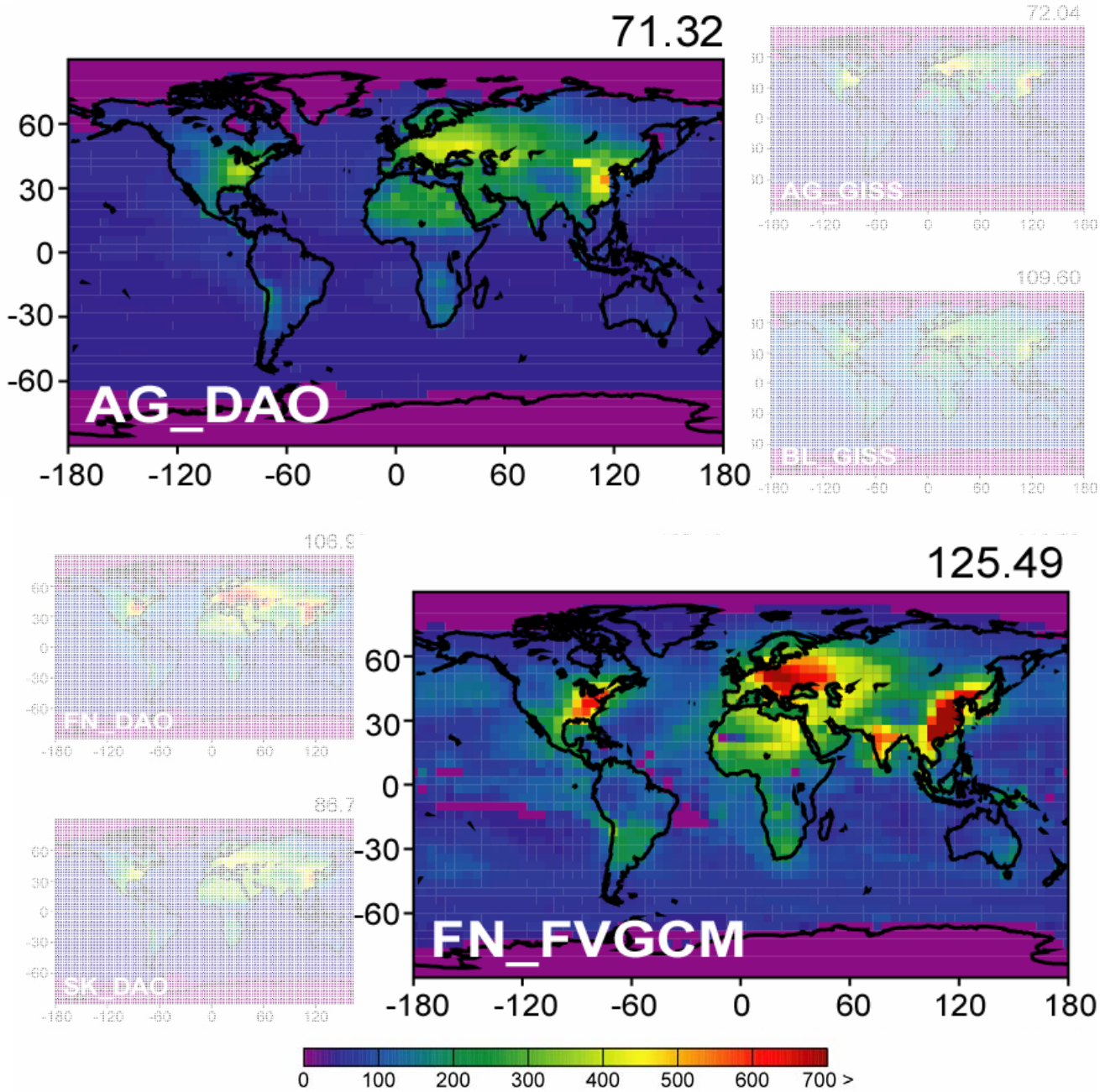

Despite the general similarity in the spatial patterns, there are considerable differences introduced by different meteorological fields and droplet activation parameterizations

Droplet Effective Radii (μm)

Maximum droplet size is calculated over the western tropical Pacific warm pool region, where large evaporation associated with large sea surface temperature exists.

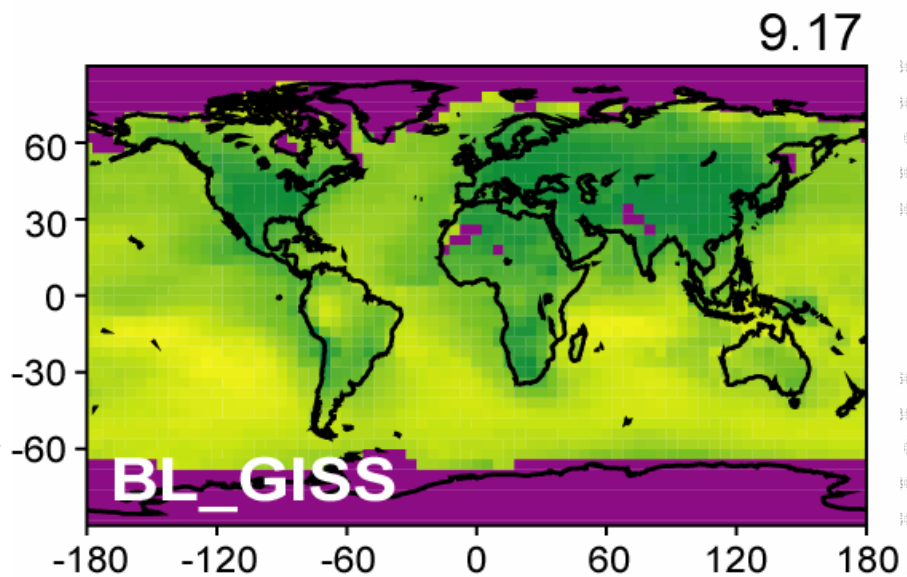

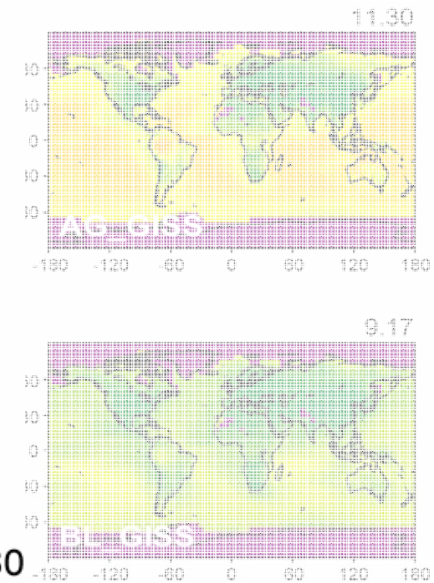

The smallest effective radius is calculated over continental regions with enhanced CCN concentration (i.e., eastern China, North America and Western Europe)

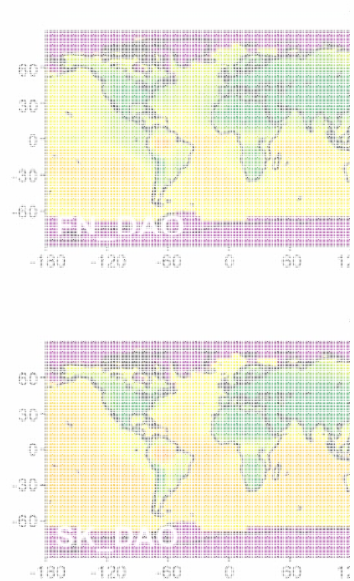

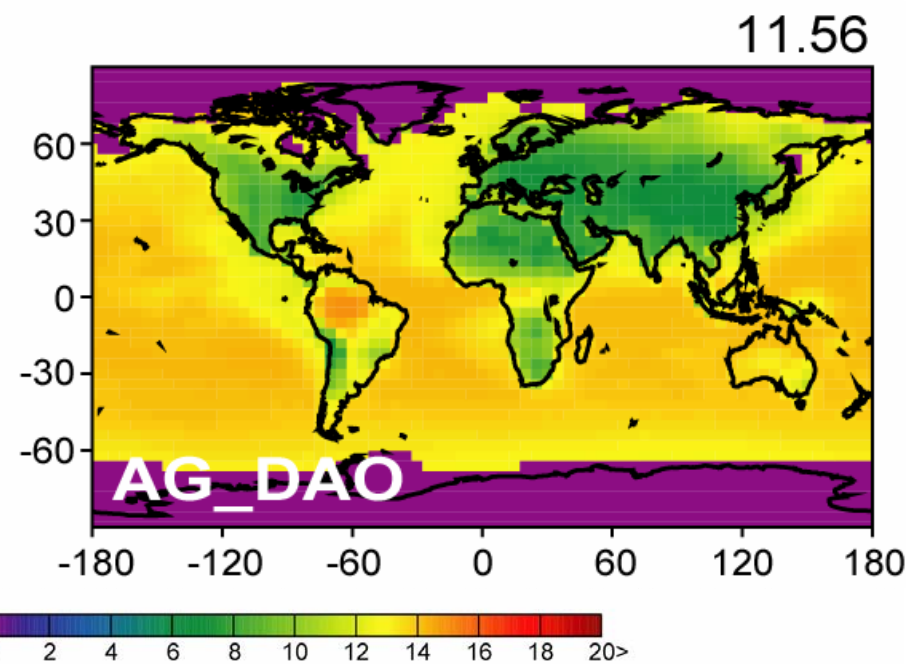

Cloud Optical Thickness (τ)

Higher COD is predicted for the clouds over anthropogenically influenced regions of eastern China, Europe, eastern US, and some biomass burning regions in South America and West Africa.

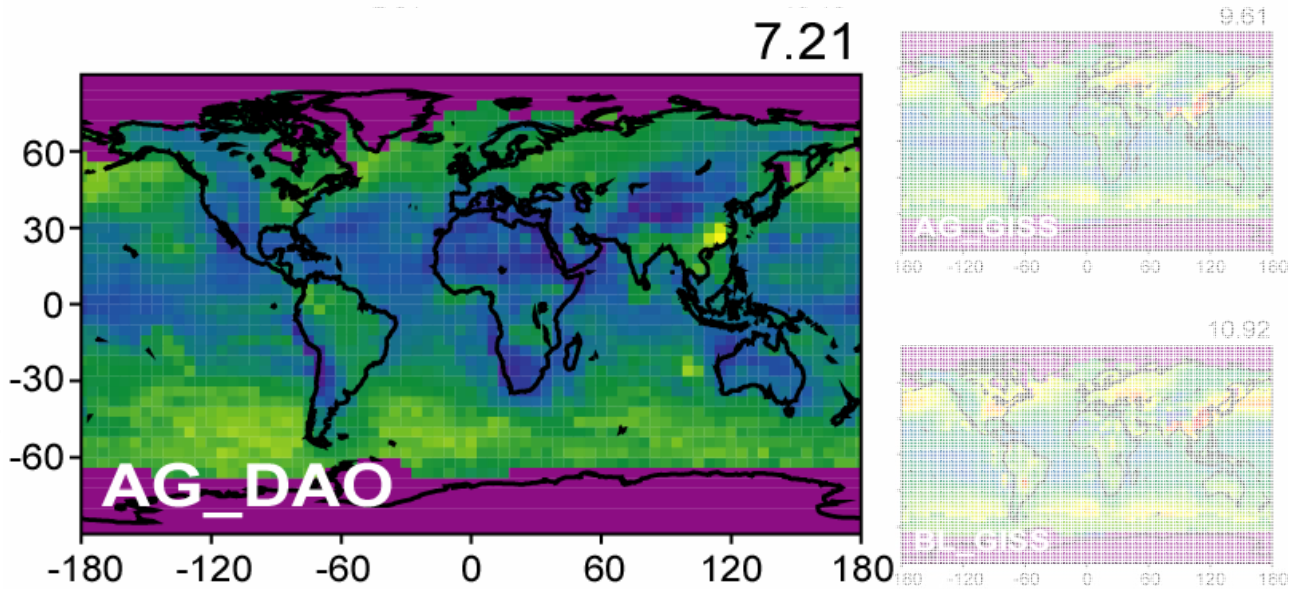

Different metfields contribute 70% variability in globally averaged COD. Results from different cloud droplet activation parameterizations contribute a variability of 30%

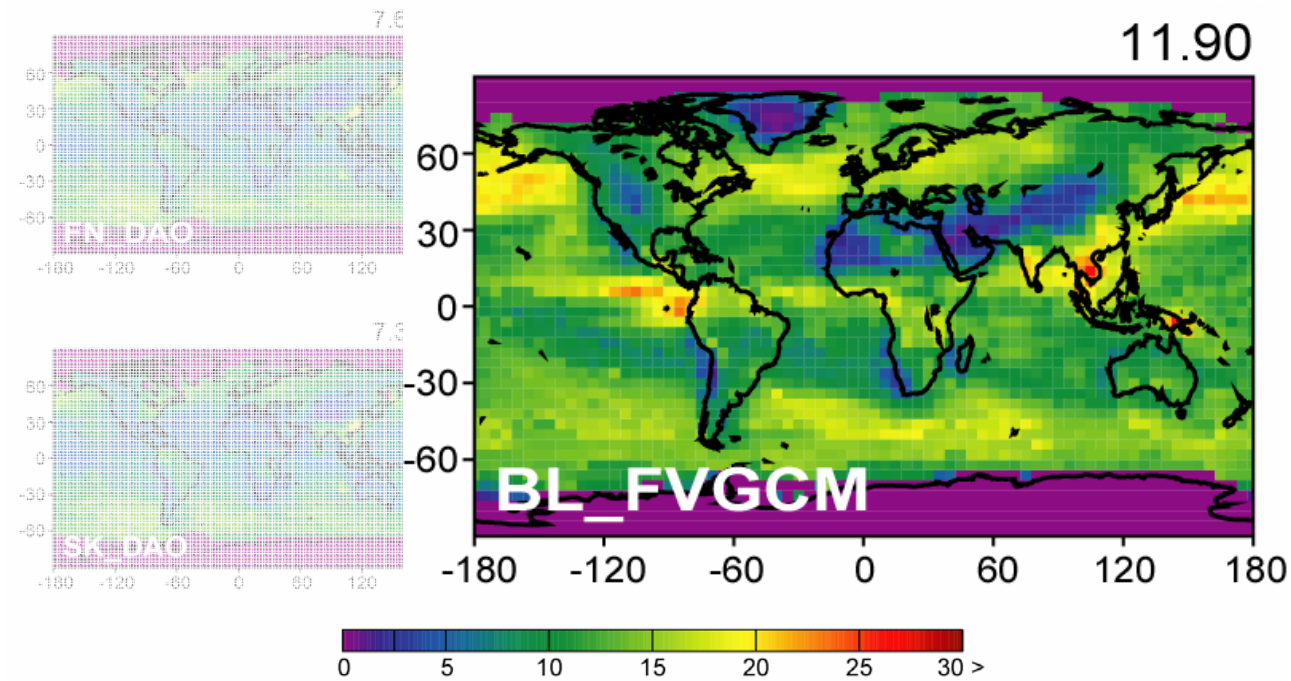

Annual Mean First Indirect Effect (W m^{-2})

Spatially, there are strong horizontal inhomogeneities with the largest values of AIE predicted over SE Asia, Western Europe and Eastern US (i.e., areas with highest amount of anthropogenic sulfur emissions)

Different meteorological datasets are predicted to contribute 38% variability in globally averaged AIE, while results from different cloud droplet formation parameterizations contribute a variability of 62%

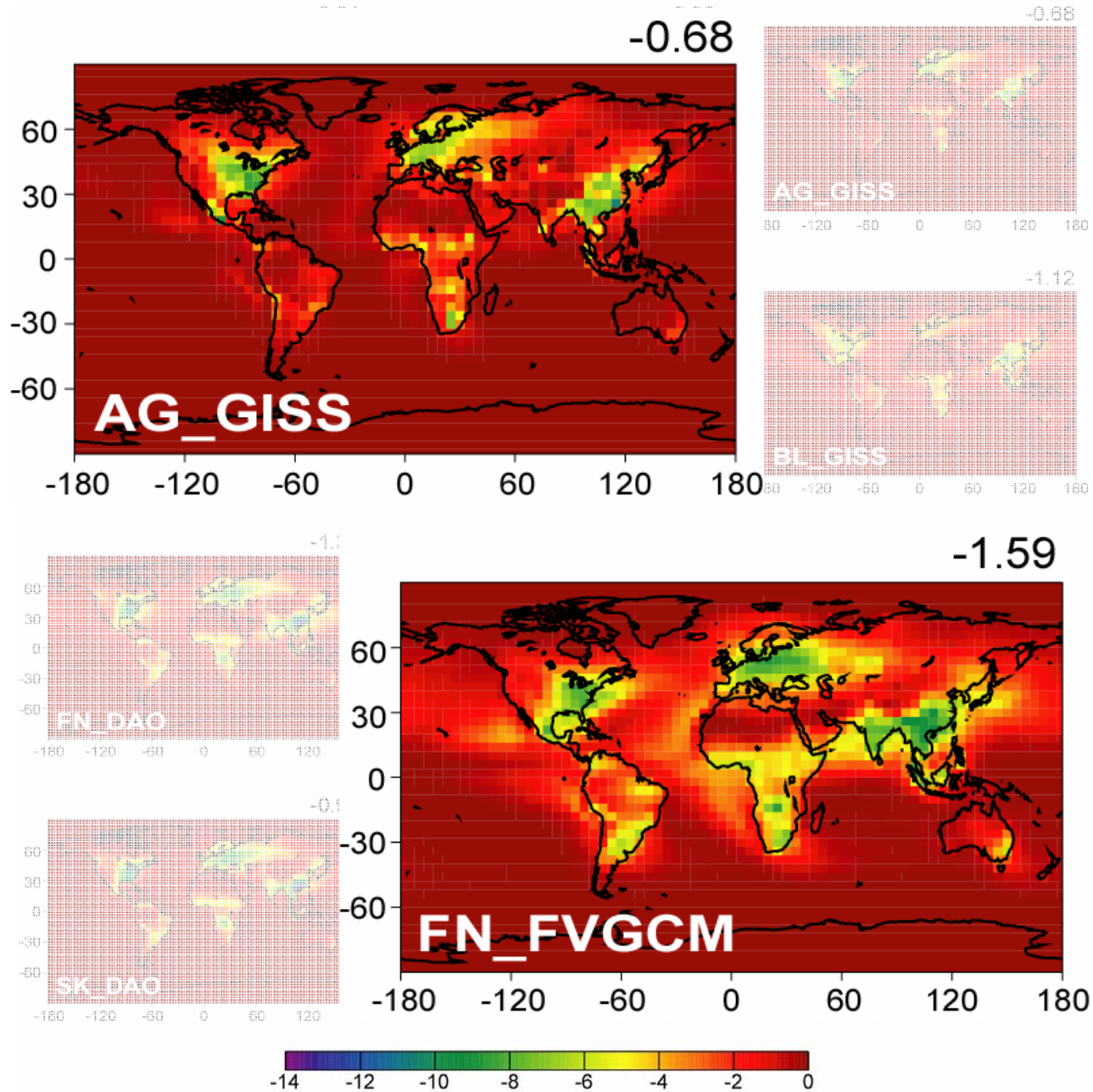

Annual Mean Autoconversion Rate ($\times 10^{11}$ s^{-1})

Conditions: Eq.1 of Kharoutdinov and Kogan, 2000

The contrast between land and ocean is large.

Different meteorological fields contribute 70 % variability in calculations of autoconversion.

Cloud droplet formation schemes are of lesser importance for autoconversion rate calculations.

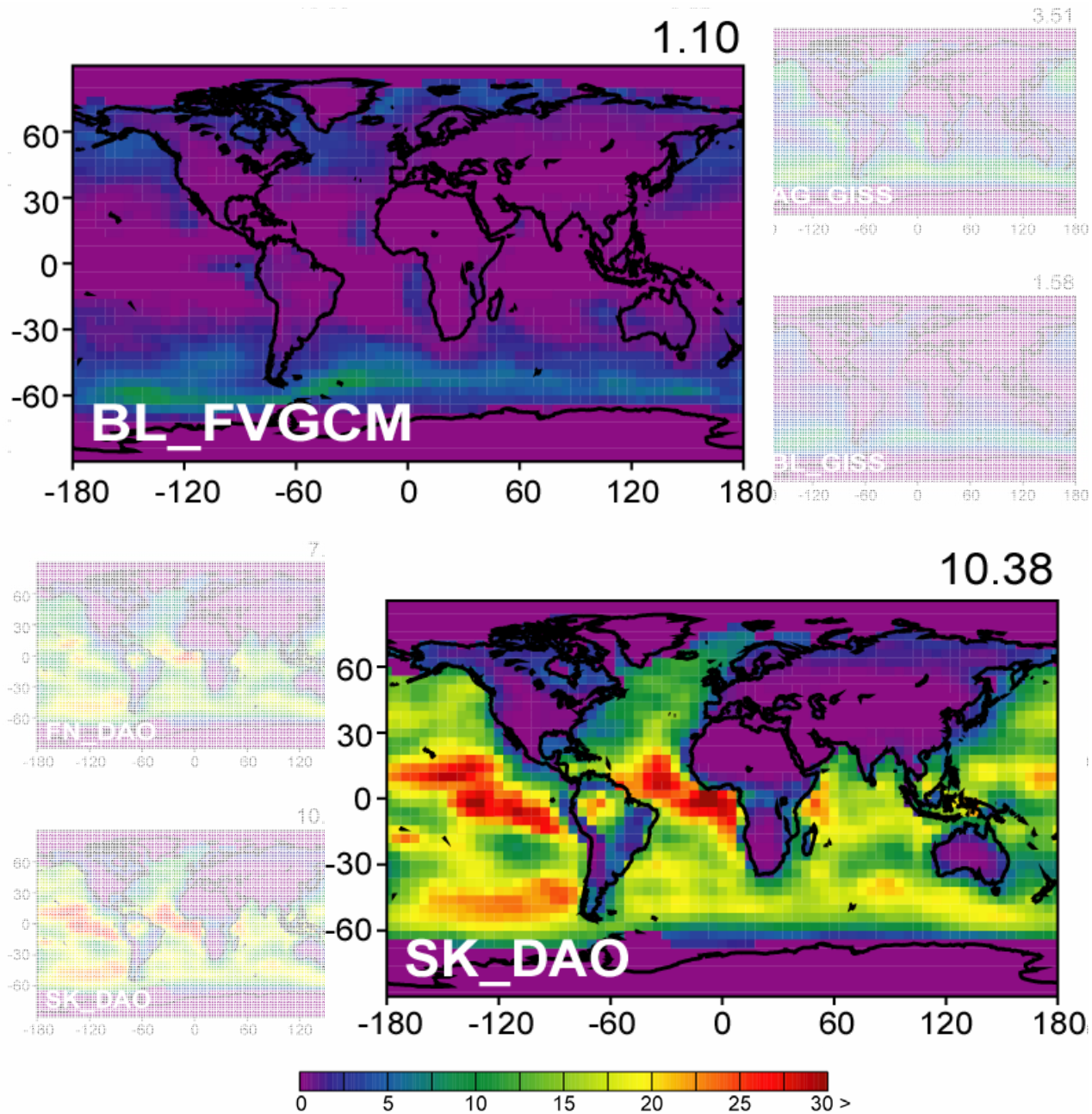

Annual Mean Autoconversion Forcing

Let's define a new concept, similar to indirect radiative forcing, but is more appropriate for precipitation change tendencies.

We call this "autoconversion forcing" and it represents the change in autoconversion rate (without any feedbacks) from the anthropogenic aerosol perturbations.

Presindustrial Autoconversion

Present day Autoconversion

$$F_A = \frac{A^{PI} - A^{CD}}{A^{PI}}$$

Autoconversion Forcing

Of course, we still need the response function, but a full climate model is needed (we will do this with the GISS)…

Annual Mean Autoconversion Forcing (%)

Conditions: Eq.1 of Kharoutdinov and Kogan, 2000

Large forcing over the continents and the ocean of the NH coinciding spatially with regions affected by pollution plumes or long range transport of pollution plumes.

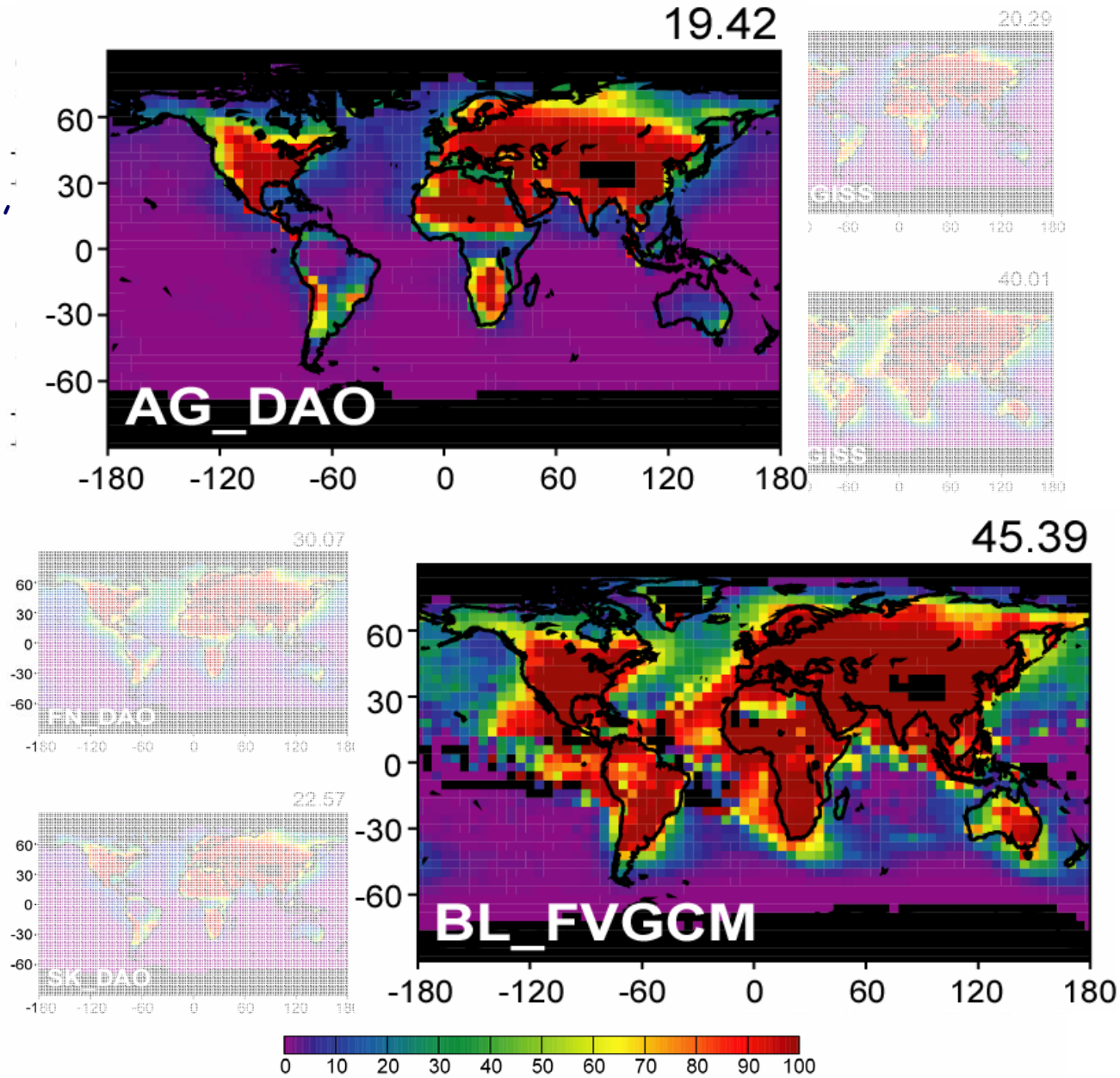

Difference in Annual Mean Autoconversion Rate Between BL and the Other Schemes

Present day autoconversion predicted by a scheme (i.e., AG, FN or SK)

Present day autoconversion predicted by BL

$$\Delta A_i = \frac{A_i^{PD} - A_{BL}^{PD}}{A_{BL}^{PD}}$$

Similar patterns for all metfields.

Large differences over the oceans; this is one of the most important source of uncertainty from the droplet schemes.

This means in the "red" areas we need to do a much better job in computing autoconversion.

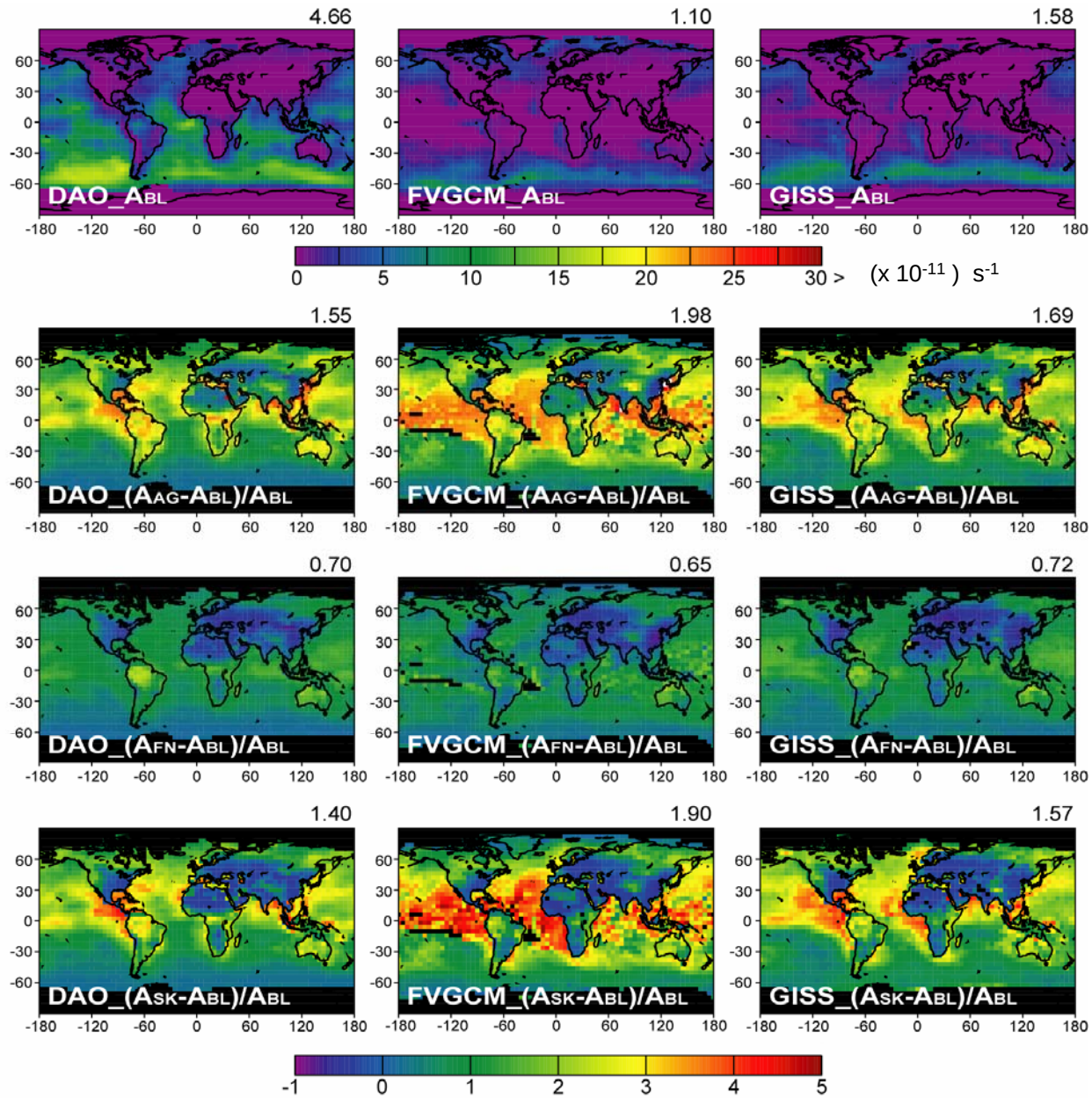

AEROCOM simulations

Conditions: GISS metfields, FN activation scheme, Liquid cloud temperatures above 263 K over land and 269 K over ocean

Similar patterns for all properties with the modeling outputs using the emission inventory of the University of Michigan, FN scheme and GISS metfield.

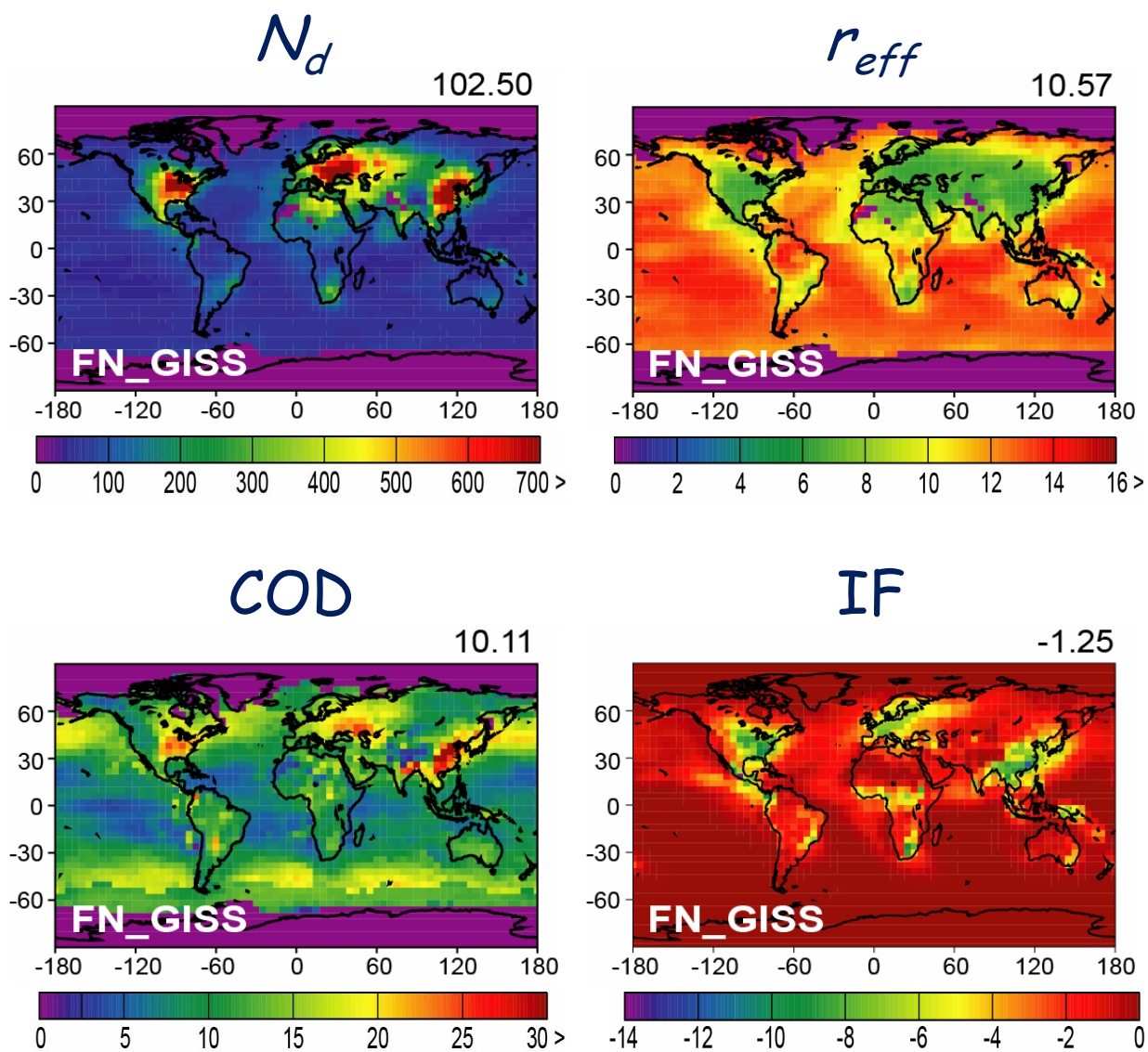

Computational requirements

- BL_DAO: 1 week ☹
- SK_DAO: 1 week + 20 min ☺
- AG_DAO: 1 week + 45 min ☺
- FN_DAO: 1 week + 60 min ☺

BL_GISS: 3 days, BL_FVGCM: 6.5 days

This ***shatters*** the common GCM dogma that "Mechanistic Parameterizations (FN) are too slow to be implemented in GCMs"

Implications and Conclusions

- GMI is able to correctly capture the land-ocean contrast in COD and r_{eff} and the spatial variations in cloud properties between the SH and the NH regions observed in remotely sensed data.
- The GMI aerosol simulation with offline GISS winds remarkably reproduces the characteristics of the online GISS (mass-only aerosol simulation).
- Depending on the droplet activation parameterization and the metfield used, global annual indirect forcing ranges:

-0.99 to -1.48 W m^{-2} for the "Base Case"

-0.68 to -1.59 W m^{-2} for all runs considered to date

Implications and Conclusions

- Different metfields lead up to **38%** (Global average) variability in indirect forcing calculations.

- Diagnostic and empirical parameterizations contribute up to **62%** (Global average) variability in indirect forcing. Although important it is a low estimate (it becomes larger if you use interactive microphysics - our experience with CACTUS and CACTUS/TOMAS support this).

- For all droplet activation parameterizations and the metfields used the global annual autoconversion rate ranges from 1.10×10^{-11} to 10.38×10^{-11} s^{-1} . The metfields contribute 70% variability and 30% is from the activation parameterization.

Implications and Conclusions

- The spatial patterns of autoconversion rate are similar for all metfields.
- Large differences in autoconversion rates over the oceans; this is one of the most important source of uncertainty from the droplet schemes.
- Larger autoconversion forcing (60-100%) is predicted over the anthropogenically perturbed regions of the globe

Work in Progress – Future Plans

- Run the indirect & autoconversion forcing simulations for interactive aerosol microphysics. (Joyce)
- Use GISS-TOMAS to extract look-up tables (monthly averages) of the aerosol size distribution and standard deviation as a function of time and place and use them in GMI to calculate indirect & autoconversion forcing.
- Introduce the entraining cloud droplet formation parameterization that we have developed in the group (Barahona and Nenes, *JGR, in press*)
- "Tie" autoconversion with cloud droplet formation even better.

Work in Progress – Future Plans

- Cloud spectrum parameterization (Hsieh and Nenes, *in prep*) to link autoconversion with activation; reduce the need for "tuning" autoconversion parameterizations.
- Examine the potential effect of organic compounds on CCN formation (using the "insoluble" fraction of the aerosol).
- Assess the uncertainty in cloud droplet number, indirect radiative forcing and autoconversion rate associated with application of Köhler theory.
- Explicit calculation of the effective radius and the indirect forcing from "k"– Examine the sensitivity to met-fields and droplet formation parameterizations.
- … and the list goes on.

Ongoing projects in the group of potential interest to GMI

(Jose, can we have a few more minutes?)

Assess the indirect forcing uncertainty arising from application of Köhler theory

Procedure:

- Use in-situ data and assess CCN closure, for various assumptions on chemical composition taken in GCMs.
- Quantify CCN prediction error
- Incorporate into GCM and assess uncertainty in
  - ✓ Cloud droplet number concentration (CDNC)
  - ✓ Aerosol indirect forcing
  - ✓ Autoconversion of cloudwater to rain

Determine regions where uncertainty is small; define regions where more in-situ constraints are needed.

CCN Prediction Uncertainty

From the ICARTT dataset

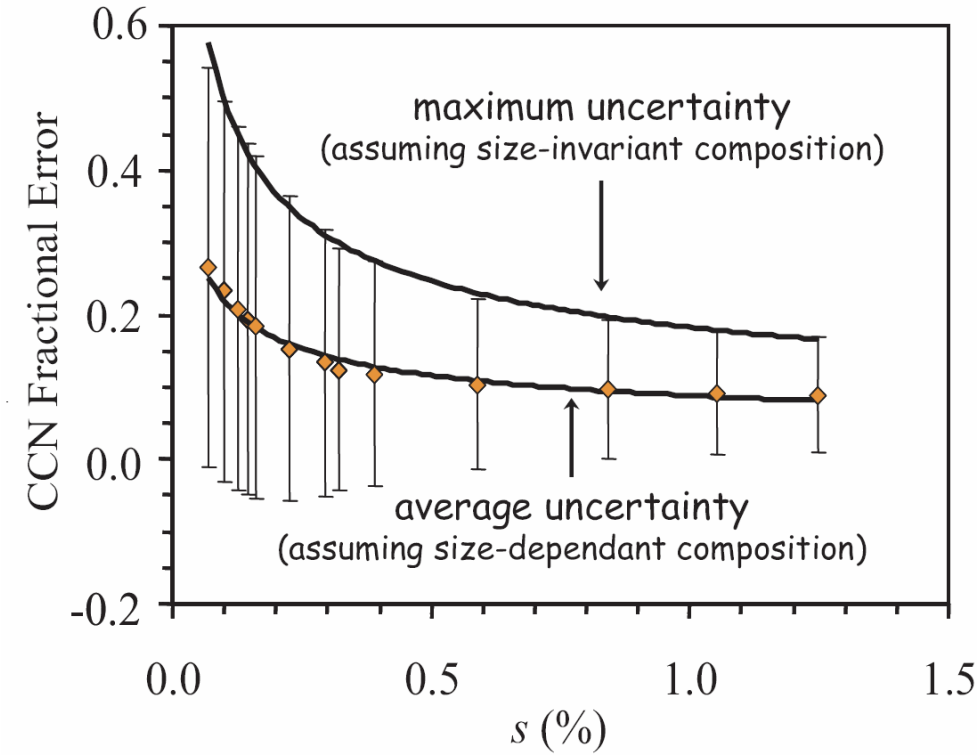

Observed CCN

Predicted CCN

$$\varepsilon_{CCN}(s) = \frac{F_o(s) - F_p(s)}{F_o(s)}$$

The prediction error decreases as supersaturation increases

Error range: 10 - 60%

We now have datasets from GoMACCs (Houston, 2006), Mexico City (2006), Finland (Hyÿtialä, 2007), Greece (Crete, 2007), Monterey, CA (2007). We will have a characterization of CCN prediction uncertainty for different locations, aerosol characteristics and seasons.

We are developing a global characterization of CCN prediction "skill"

Indirect Forcing Uncertainty

Using the ICARTT dataset in online GISS (Sotiropoulou et al., in press)

Range: 10-120% Global average: 50%

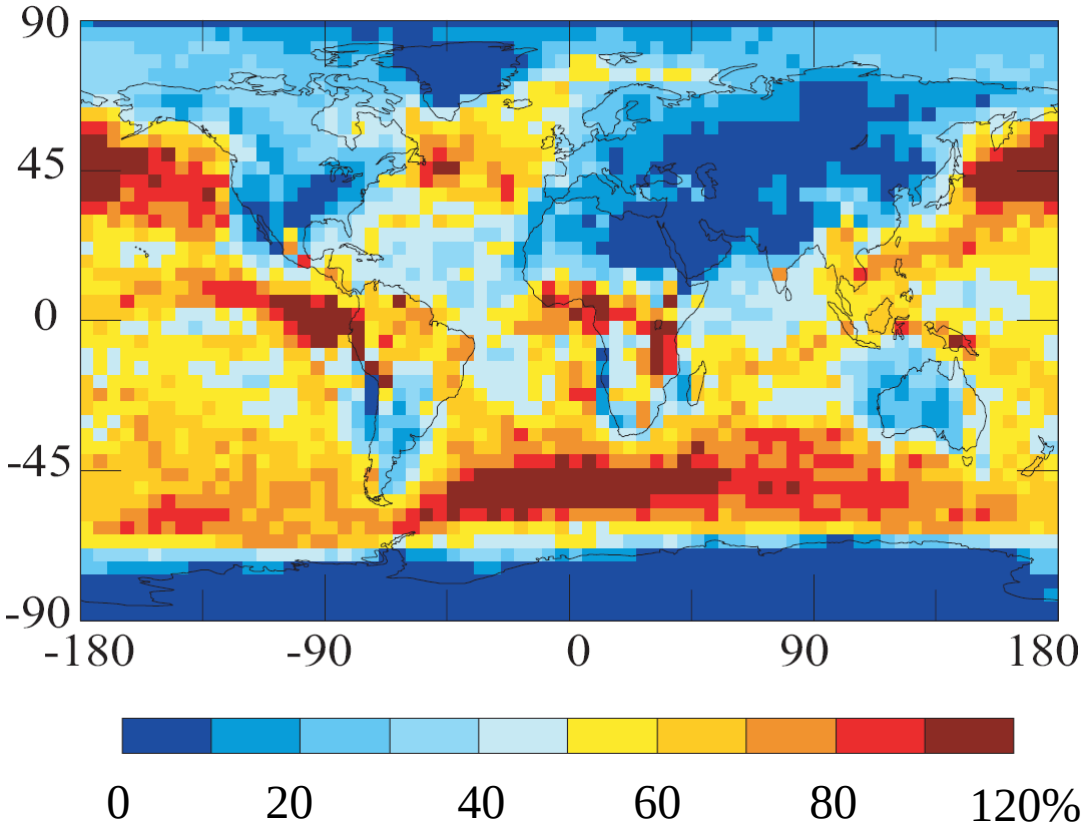

$$U_{IF} = \left| CF_{TOA}^{max^+} - CF_{TOA}^{max^-} \right|$$

Larger uncertainty is predicted downwind of industrialized and biomass burning regions

The least indirect forcing uncertainty is predicted over deserts and the subtropical southern oceans

It would be IDEAL to repeat this within the GMI for different met fields, droplet schemes and of course, with all the CCN data at hand!

ISORROPIA-II: A new thermodynamic equilibrium model for $K^+/Ca^{2+}/Mg^{2+}/NH_4^+/Na^+/SO_4^{2-}/NO_3^-/Cl^-/H_2O$ Aerosol

- Solve the full thermodynamic partitioning equations for aerosol systems with the major inorganic precursors.
- Predict aerosol phase(s), composition of each, and of course, water uptake.

Some groups using ISORROPIA

- NASA GISS Global Climate Model
- EPA Community Air Quality model (CMAQ)
- EPRI's CAMx model
- Sonoma Tech's UAM-AERO
- Meteo-France Group
- Max Planck Institute for Tropospheric Research
- University of Athens, Greece
- Ford Motors - Aachen

The "ISORROPIA II" model: Possible species

Solid phase: $NaHSO_4$, NH_4HSO_4 , Na_2SO_4 , NaCl, $(NH_4)_2SO_4$, $(NH_4)_3H(SO_4)_2$, NH_4NO_3, NH_4Cl, $NaNO_3$, **K_2SO_4, $KHSO_4$, KNO_3, KCL, $CaSO_4$, $Ca(NO_3)_2$, $CaCL_2$, $MgSO_4$, $MgCL_2$, $Mg(NO_3)_2$**

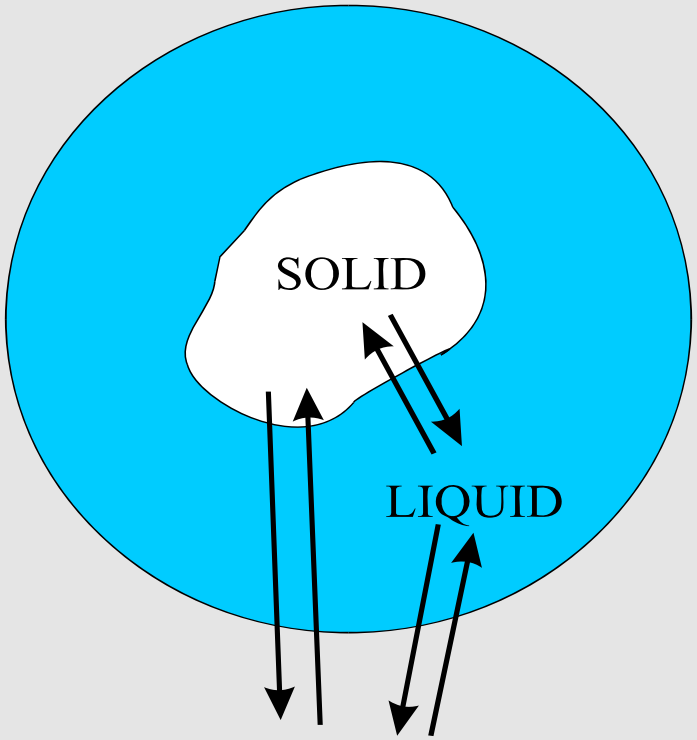

Liquid phase: Na^+, NH_4^+, H^+, OH^-, HSO_4^-, SO_4^{2-}, NO_3^-, Cl^-, H_2O, $HNO_{3(aq)}$,$HCl_{(aq)}$, $NH_{3(aq)}$, **Ca^{2+}, K^+, Mg^{2+}**

Gas phase: HNO_3, HCl, NH_3, H_2O

Species in ISORROPIA-II

New Ice Nucleation Parameterization

- Currently looking at homogeneous freezing
- Freezing of supercooled droplets, influenced by:
  - Thermodynamical and dynamical state: (RHi, T, P, updraft velocity)
  - Composition and size: their role is still not well understood
- Stochastic process
- Very rapid
- Proceeds even after S_{max} has been surpassed

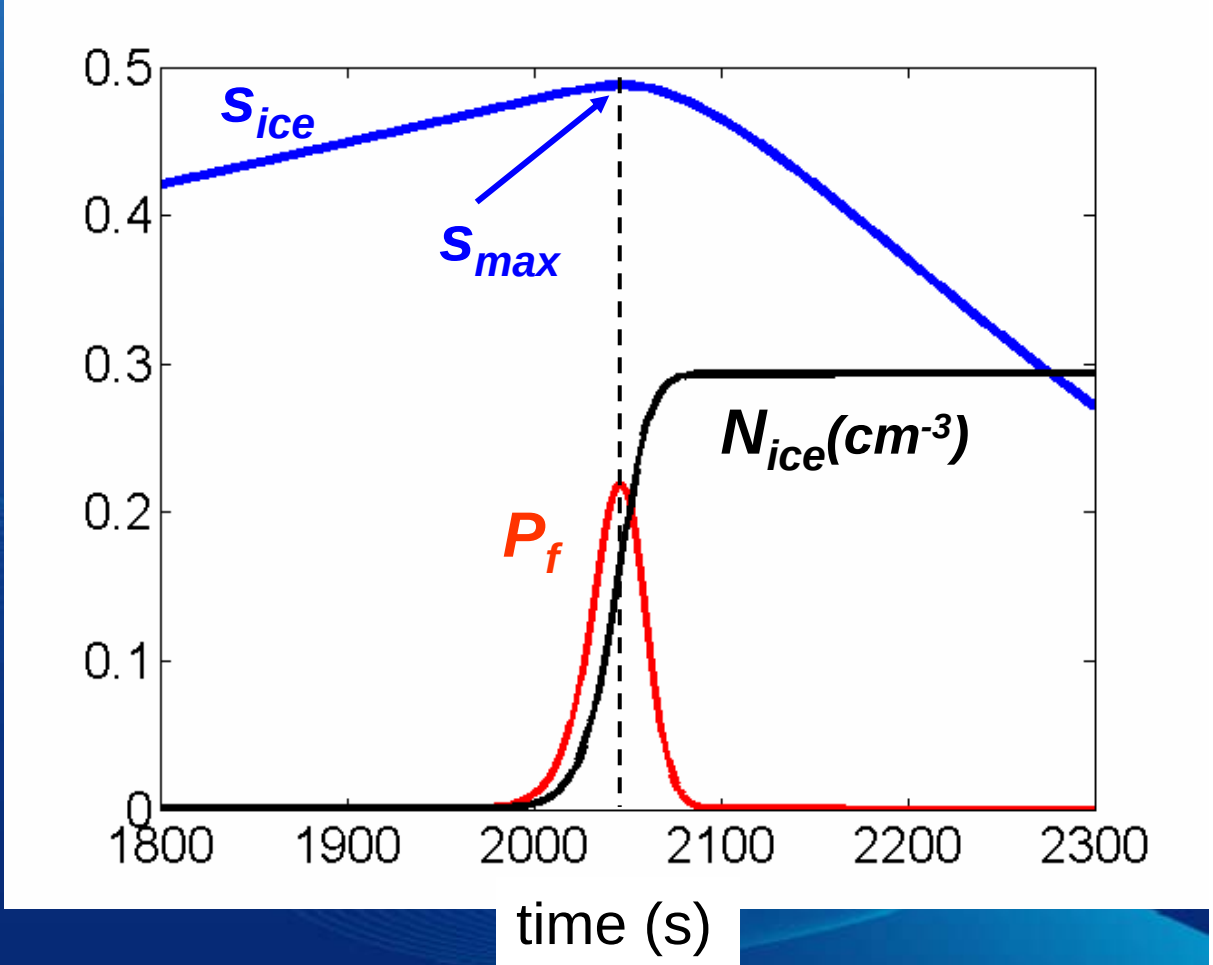

Example: parcel model simulation of cirus cloud formation. T_o=233 K, P=340 hPa, W=0.2 ms^{-1}

Barahona D. and Nenes A.,2007, *in preparation.*

Parameterizing Ice Formation

- For each ice particle we trace back its growth and find the S_i at which the freezing occurred, then we calculate $n_c(D_p, S_i)$

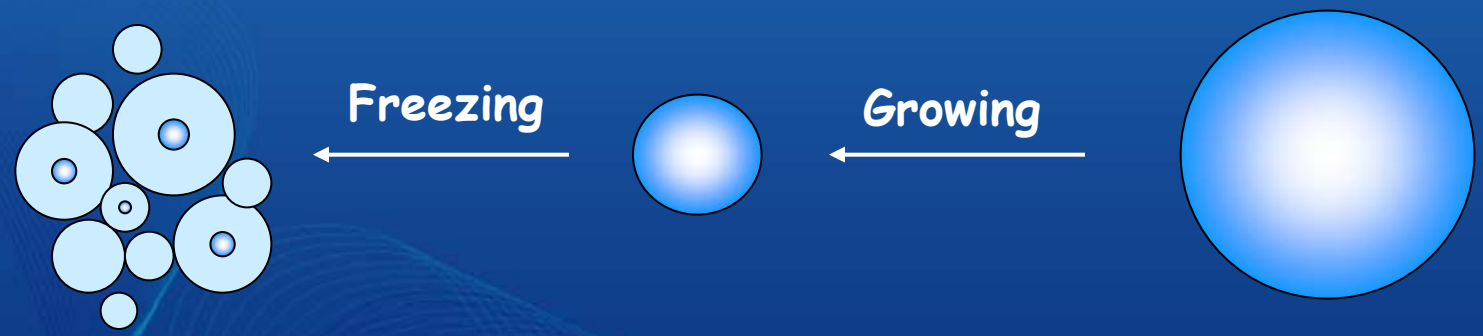

$$S_o^{'} = S_{\max}\left(1-(D_p^2 - D_o^2)*\left[\frac{\alpha\, w}{G(S_{\max}-1)}\right]\right)$$

$$n_c(D_p) = n_a(s_o^{'})*\frac{dP_f}{dD_p}(s_o^{'})$$

- We look for an asymptotic value of N_i rather than its value at S_{max}
- Based on first principles; avoid "artificial" constants (i.e., freezing time scales or constant freezing thresholds)

Parameterization: Homogeneous Nucleation

N_c (cm^{-3})

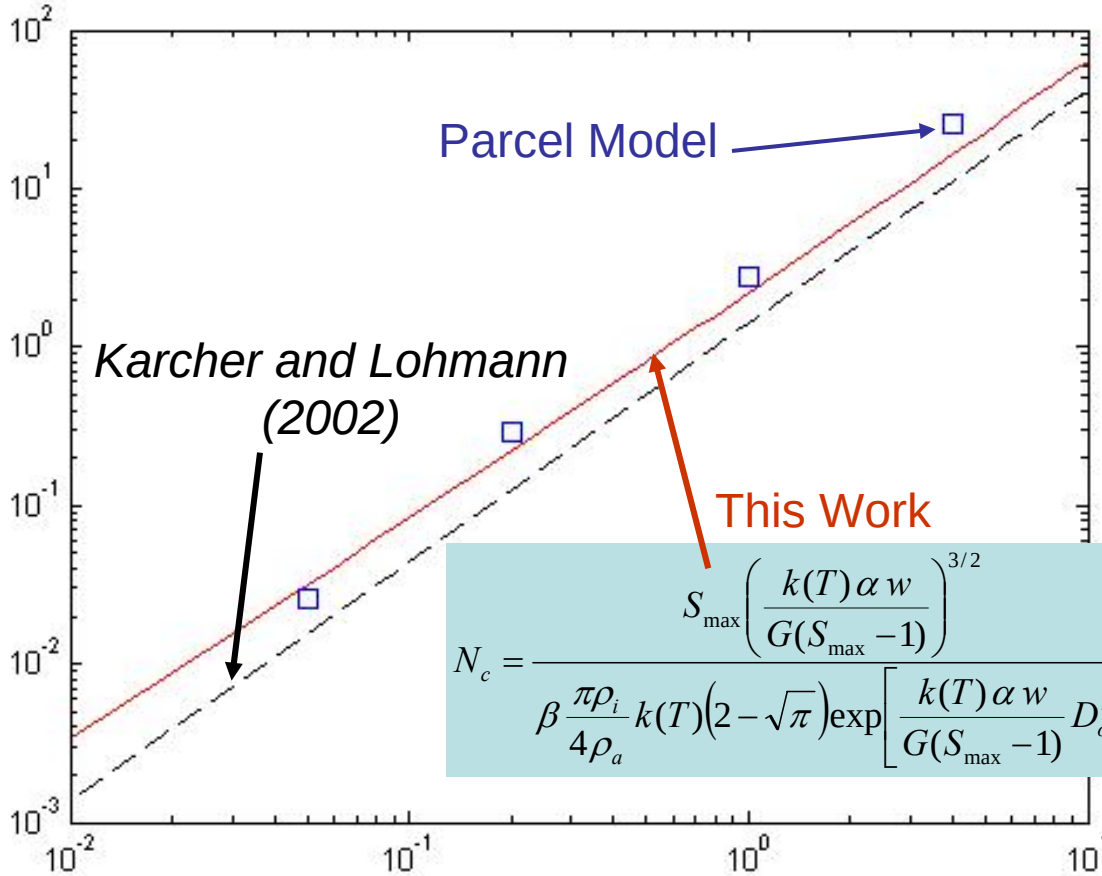

$$N_c = \frac{S_{\max}\left(\frac{k(T)\,\alpha\, w}{G(S_{\max}-1)}\right)^{3/2}}{\beta\frac{\pi\rho_i}{4\rho_a}k(T)\left(2-\sqrt{\pi}\right)\exp\left[\frac{k(T)\,\alpha\, w}{G(S_{\max}-1)}D_o^2\right]}$$

w (ms^{-1})

Example: T_o=233 K, P=220 hPa, W=0.2 ms^{-1}

Barahona D. and Nenes A.,2007, *in preparation.*

Thank you!

Supporting Material

Cloud Droplet Number (cm^{-3}) (annual average)

Conditions:

Prescribed updrafts (marine: 0.25 ms^{-1}; continental: 0.5 ms^{-1})

Water vapor mass uptake coefficient, a_c, is set to 0.06

Bulk microphysics

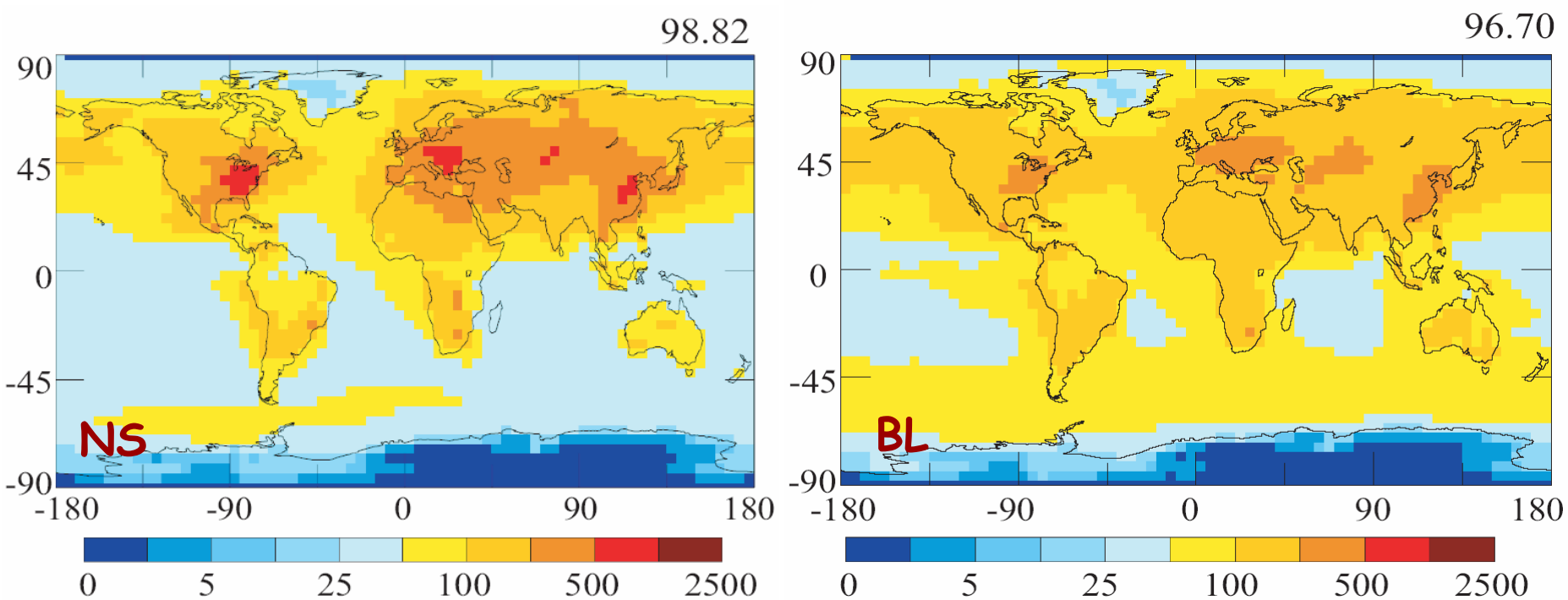

Cloud Droplet Number (cm^{-3}) (annual average)

Conditions:

Prescribed updrafts (marine: 0.25 ms^{-1}; continental: 0.5 ms^{-1})
Water vapor mass uptake coefficient, a_c, is set to 0.06
Detailed microphysics (CACTUS/TOMAS)

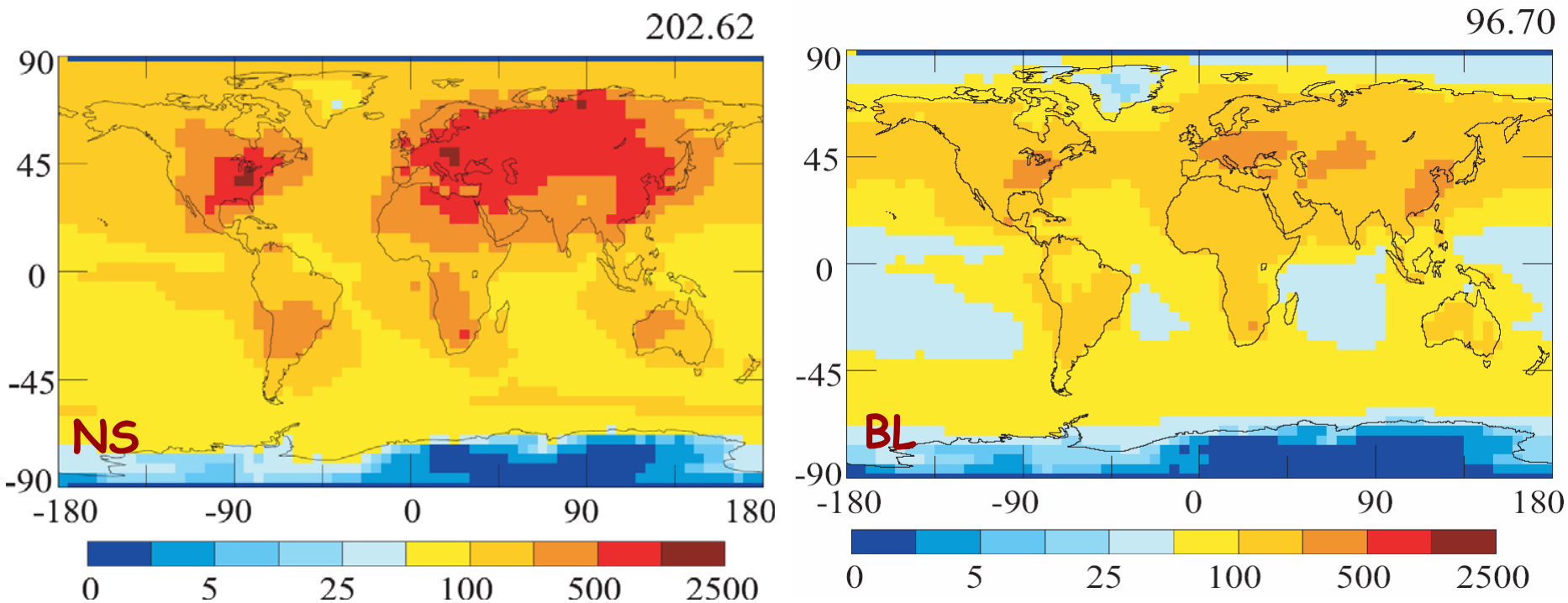

Parameterizing drizzle: how it's done now

Precipitation formation in GCMs is often *decoupled* from activation, and generation of rainwater is expressed in terms of a 'critical' liquid water content beyond which rainwater production becomes efficient:

conversion rate 'constants'

$$(\dot{q}_l)_P = -\left(c_T \left[1 - \exp\left\{ -\left(\frac{q_l / C}{c_w} \right)^2 \right\} \right] + c_A P \right) q_l$$

(Rotstayn, 1997)

critical LWC for rainwater

This is not how it happens in nature; rain is a collection process and must be treated as such, if possible.

Parameterizing drizzle: how it's done now

Improved precipitation parameterizations that consider microphysics exist, and are also used,

liquid water cloud fraction

average collection efficiency

$$(\dot{q}_l)_P = -C_1 \frac{0.104 g E \rho^{4/3}}{\mu (N_d \rho_w)^{1/3}} \left(\frac{q_l}{C_1} \right)^{7/3}$$

(Rotstayn, 1997)

droplet number

This is a step in the right direction, but the effects of spectral broadening (droplet size distribution) are not explicitly considered.

We seek an explicit link between aerosol, activation and subsequent coalescence at the "updraft" scale.

We are doing this now by predicting droplet size distribution in the updrafts that form clouds online in the GCM.

Parameterizing drizzle: what we will implement

Two-moment schemes developed for small-scale models can be used instead:

(e.g., Cohard and Pinty, 2000; there are more like R4 and R6 schemes of Liu & Daum)

spectral dispersion *average droplet size*

$$(\dot{q}_l)_P = -\frac{2.7\times10^{-2}\rho q_c\left(\frac{1}{16}\times10^{-20}\sigma^3 D_v - 0.4\right)}{\frac{3.7}{\rho q_c}\left(0.5\times10^6\sigma - 7.5\right)^{-1}}$$

We have all the elements we need (dispersion, droplet size) for a comprehensive treatment of precipitation. Why not include it in the GCM?

Challenge: How do we obtain these parameters in the global model?

Solution: From the *Nenes and Seinfeld Activation Parameterization*

Parameterizing drizzle: predicting droplet size in GCMs

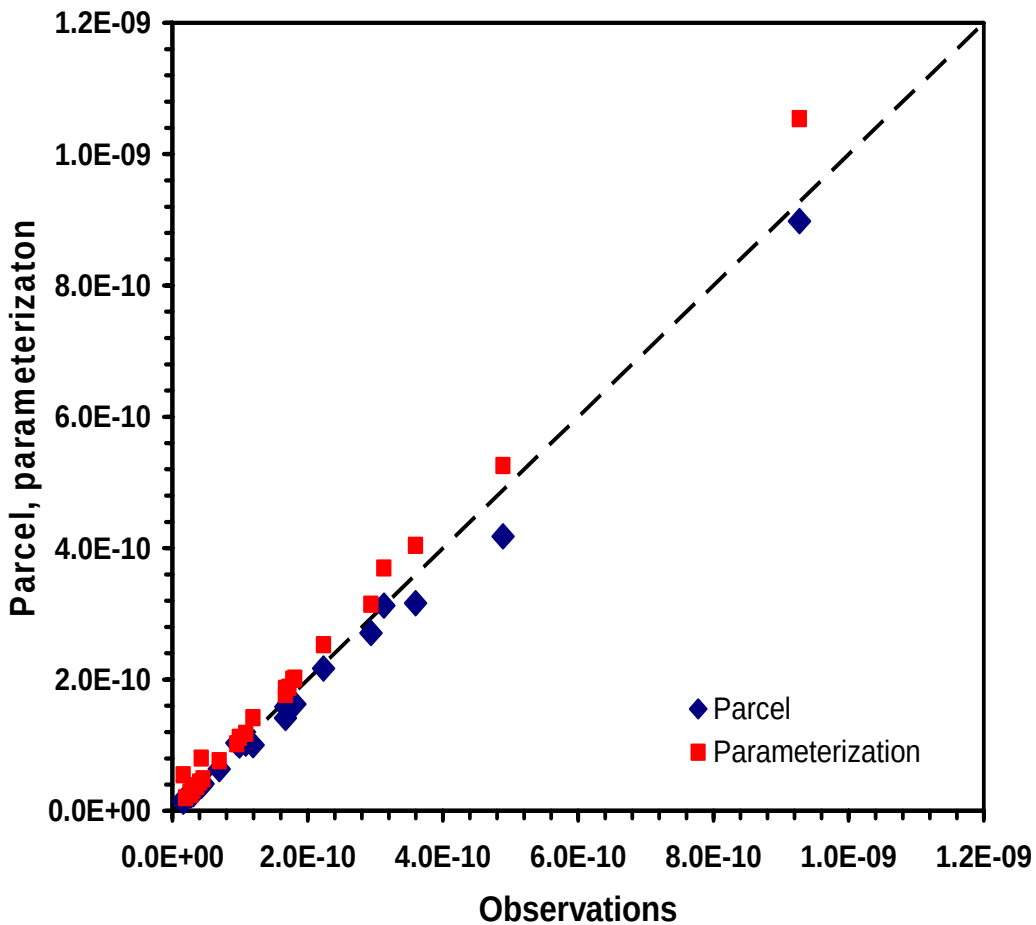

- Predict size distribution with Nenes and Seinfeld parameterization and cloud parcel model for **adiabatic cases** of CRYSTAL-FACE (cumulus) clouds.
- Use droplet number & size distribution to predict autoconversion rate.
- Use in-situ data to calculate autoconversion as well.
- The parameterization (and parcel model) capture the spectral width for adiabatic clouds well.
- Is it always like this? No.
- We need to address this problem.

Hsieh and Nenes, *in prep.*

Droplet size distribution and effects of entrainment

- Aim to predict droplet size distribution directly from our parameterizations; this would allow explicit computations of r_{eff} and autoconversion.
- **Current parameterizations are adiabatic**. Clouds are generally not.
- This affects primarily the computation of size (adiabatic gives too narrow distributions).

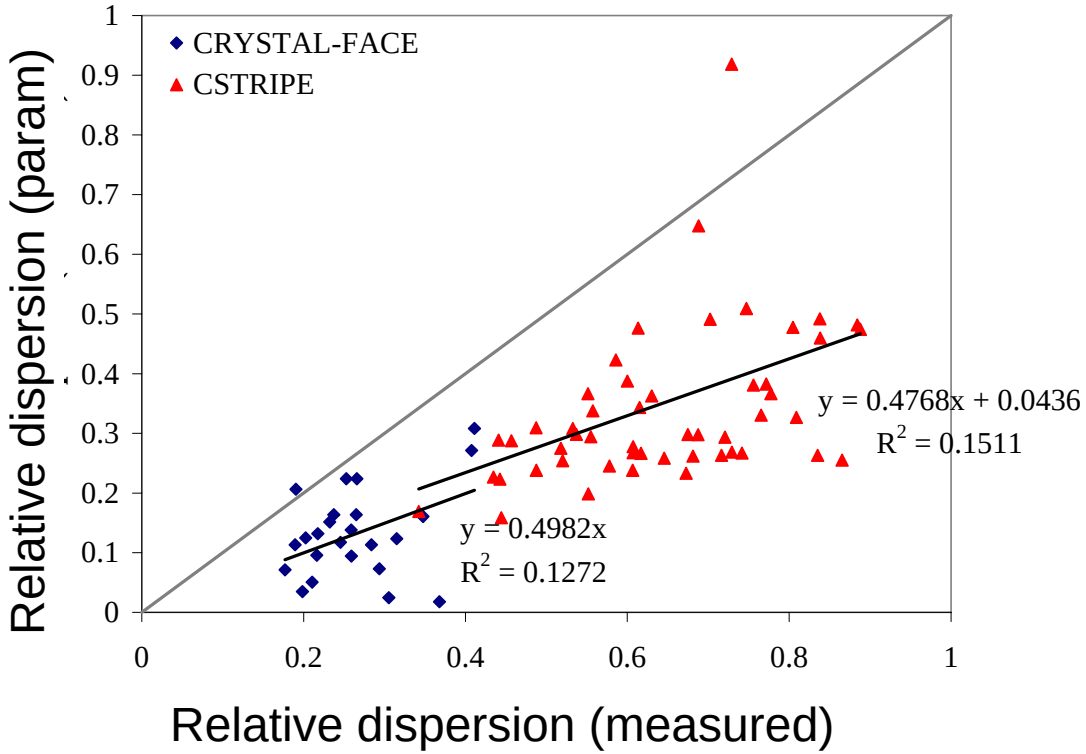

- Relative dispersion as predicted by Fountoukis and Nenes (2005) parameterization vs. *in-situ* data.
- Parameterization and cloud parcel model are in excellent agreement, but underpredict dispersion by a factor of two.
- An entraining parameterization would improve this because entrainment broadens the distribution.

Entraining cloud parameterization (Barahona and Nenes, JGR, in press)

- The first parameterization of its kind.
- Complex organics can be treated, same conceptual framework ("population splitting") as the adiabatic parameterization.
- Mixing is parameterized in terms of an entrainment rate.
- Versions for lognormal and sectional aerosol developed.
- **Same CPU requirements as the adiabatic "version".**

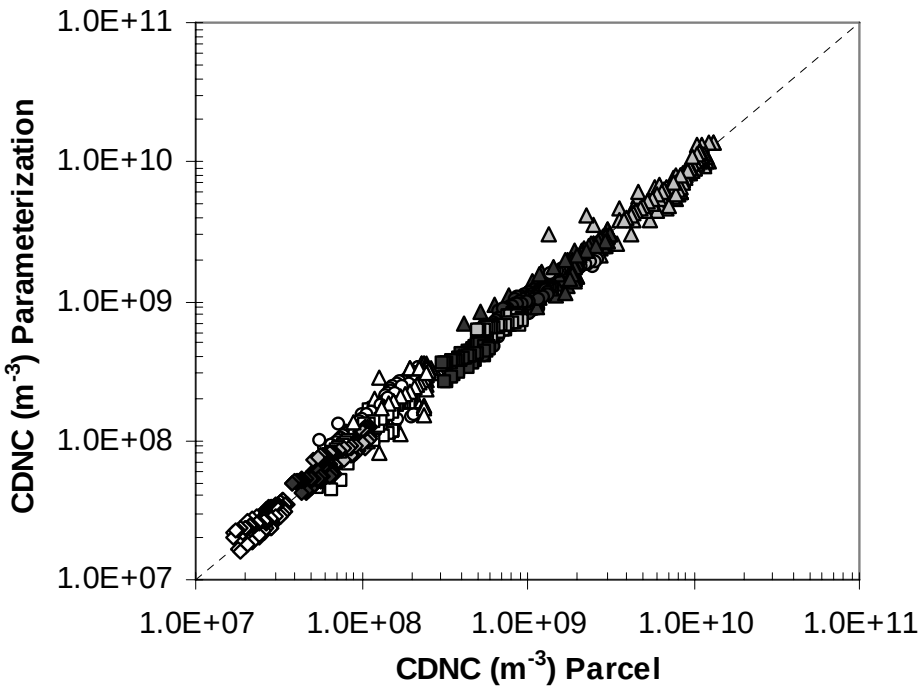

We've looked at 4000 cases
Average error:10%

We plan to use CRYSTAL-FACE, CSTRIPE, ICARTT, MASE, TEXAS-AQS data to constrain the entrainment rate.

The predicted in-cloud droplet size distribution will be evaluated with the same dataset.

New cloud droplet formation parameterization (Includes entrainment)

Why need a new parameterization?

- **Current parameterizations are adiabatic**. Clouds are generally not.
- Droplet number predictions are good even for slightly diabatic conditions (although N_d can still be overestimated for strong entrainment).
- Nenes and Seinfeld can predict droplet size distribution, but they are too narrow (adiabatic), so autoconversion calculations would generally be "off".

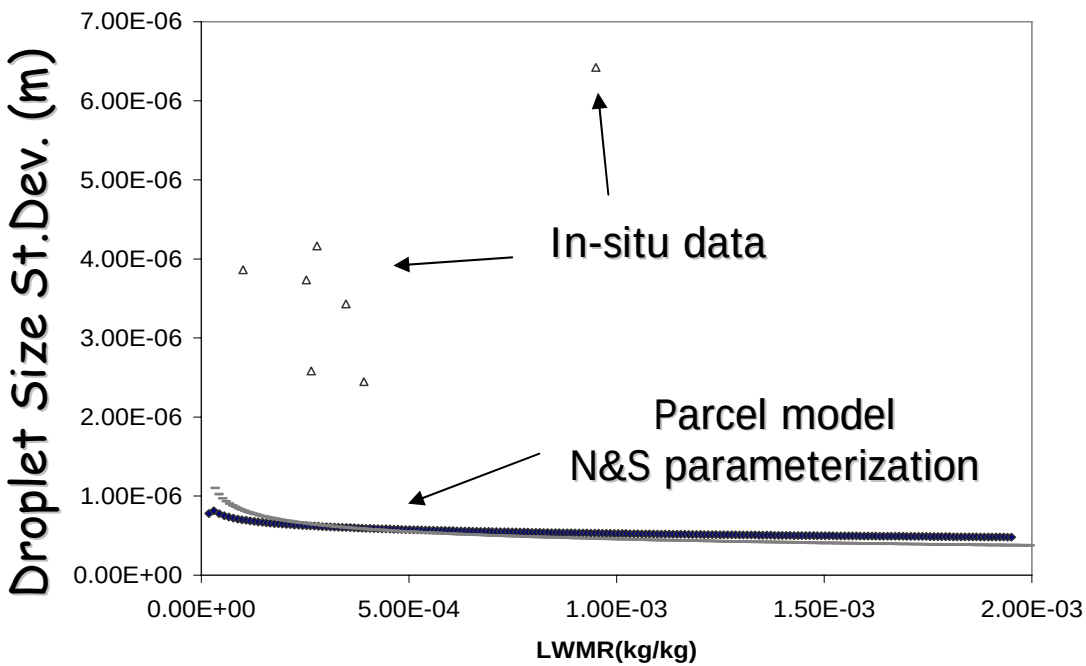

- Comparison of predicted size distribution "width" vs. liquid water content for non-adiabatic CRYSTAL-FACE (cumulus) clouds.
- Parameterization and cloud parcel model agree great with each other, but not with the data (even though cloud droplet number is captured to within 5%!).
- An entraining parameterization would improve this because entrainment broadens the distribution.

Conceptual model for Ice Formation

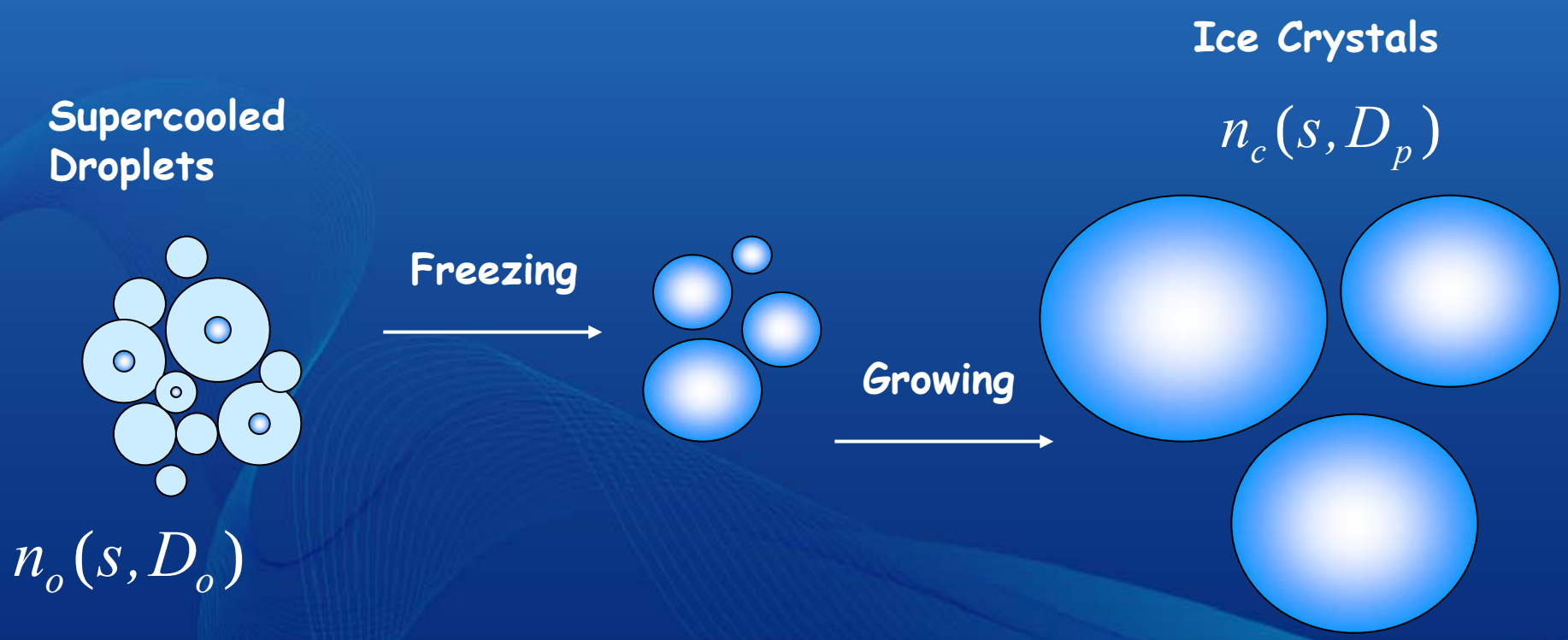

- Droplets freeze in groups at the same supersaturation, s_o', and grow defining the crystal size distribution, $n_c(s, D_p)$
- The fraction of frozen droplets is determined by the probability of freezing $P_f(s_o')$

Parameterization Algorithm

Initial guesses

$$N_{ice}^{est} = \frac{4\rho_i p_a M_w}{\pi \rho_a p_i^0 M_a}\left(\frac{\alpha w}{G}\right)^2 \qquad s = 1.01 * s_o$$

Increase s

Correct N_c

$$N_{ice} = \overline{n_a}\int_{C_S} \frac{dP(s, D_o)}{ds} ds = ?\, N_c^{est} \rightleftarrows N_c^{est} = N_c$$

No

yes

Correct s

$$P_f(s) = 1 - \exp\left(-\int_{C_S} \frac{J v_o}{ds/dt} ds\right) \leq ?10^{-6}$$

No

yes

Output: N_c, s

We count the number of crystals, N_{ice}, until some supersaturation, *s*, is reached at which the freezing pulse is over

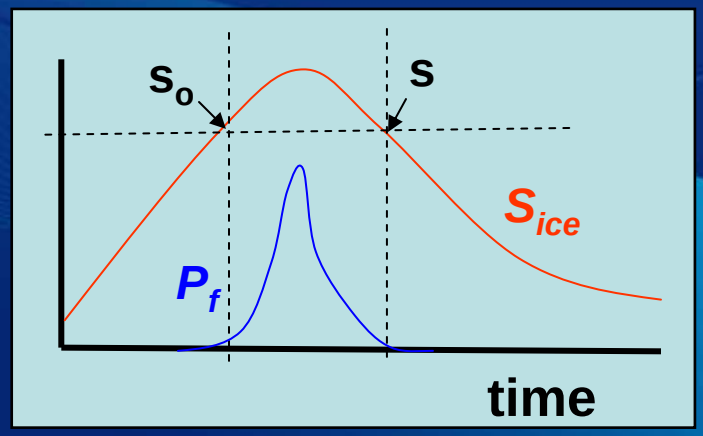

Modeling Framework

- Aerosol module (Liu et al., 2005) coupled to GMI advection core
- Emissions: SO_2, DMS, BC, OC, mineral dust, and sea salt
- Chemical production of sulfate, gravitational sedimentation, dry deposition, wet scavenging in and below clouds, and hygroscopic growth
- In cloud Liquid Water Content (Hack, 1998)
- Stratiform and Convective cloud fractions (Sundqvist et al., 1978; Xu and Krueger, 1991)

$$C_{LS} = 1 - \sqrt{1 - \frac{RH - RH_c}{1 - RH_c}}$$

$$C_C = \begin{cases} c_0 + c_1 \log(M_C) + c_2 (\log(M_C))^2 \\ \qquad \text{if } M_C > 0.01\,\text{hPa h}^{-1} \\ 0, \text{otherwise} \end{cases}$$

$$C = 1 - (1 - C_{LS})(1 - C_C)$$

Feng et al. [2004]

$$\tau = \tau_C C^{3/2}$$

Approximate random overlap (RAN) assumption
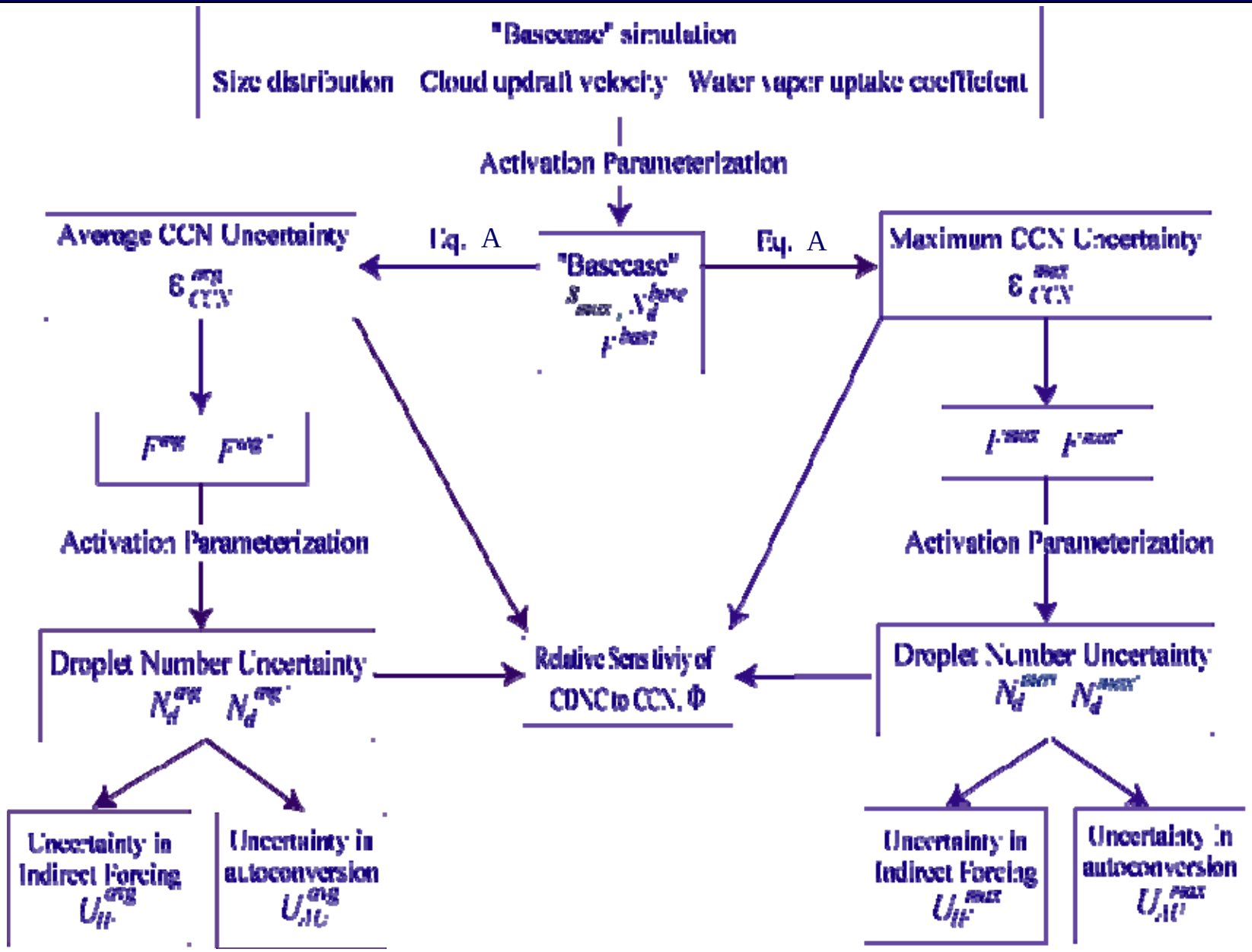
Methodology